Myosteatosis and Type 2 Diabetes Mellitus

Lucian Batista de Oliveira[1,2,*], Vanessa de Oliveira e Silva[2], Ítalo Caio Lopes Jucá[2], João Victor Gonçalves dos Santos Torres[3], Maria Roseneide dos Santos Torres[2], Fabio Moura[4], Francisco Bandeira[1]

ABSTRACT

Myosteatosis refers to the infiltration of fat into skeletal muscle tissue, being influenced by factors such as advanced age and overweight, which increase the inability of adipocytes to store lipids. This condition not only alters the structure of the muscle but is also associated with endocrinological imbalances such as insulin resistance (IR) and hyperinsulinemia, increasing the risk of developing type 2 diabetes mellitus (T2DM) and cardiovascular diseases. Computed Tomography (CT) and Magnetic Resonance Imaging (MRI) are effective methods for measuring myosteatosis, identifying areas of fat accumulation that may indicate specific regional patterns. This review aimed to evaluate the main evidence that associates myosteatosis with T2DM, compiling the epidemiological data already available on the subject and the main gaps in the literature. Ten observational studies were selected, from different regions of the world, which showed a relationship between myosteatosis and a higher incidence of T2DM, as well as IR, worse glycemic status, increased inflammatory mediators and a tendency to coronary artery disease. In conclusion, myosteatosis and T2DM are conditions with a relevant relationship and that have significant implications for public health, requiring greater standardization of myosteatosis assessment methods and interventional studies that address potential therapeutic strategies for this condition.

KEYWORDS

Diabetes Mellitus, Type 2; myosteatosis; myoskeletal lipid infiltration

AUTHOR AFFILIATIONS

[1] Division of Endocrinology and Diabetes, Agamenon Magalhães Hospital, Faculty of Medical Sciences, University of Pernambuco (UPE), Recife, Brazil
[2] Medical School of Universidade Federal de Campina Grande (UFCG), Campina Grande, Brazil
[3] Faculty of Medical Sciences, Unifacisa, Campina Grande, Brazil
[4] Endocrinology and Diabetes, University of Pernambuco, Recife, Brazil
* Corresponding author: Division of Endocrinology and Diabetes, Agamenon Magalhães Hospital, Faculty of Medical Sciences, University of Pernambuco, Recife, Brazil. Medical School of Universidade Federal de Campina Grande, Campina Grande, Brazil; e-mail: lucian.batista@upe.br

Received: 5 March 2025
Accepted: 9 August 2025
Published online: 6 October 2025

Acta Medica (Hradec Králové) 2025; 68(2): 37–44
https://doi.org/10.14712/18059694.2025.17

INTRODUCTION

Sarcopenia can be defined as a progressive and generalized disorder of skeletal muscle, where there is a gradual loss of strength and functionality, being more frequent in the elderly, but it can occur in younger individuals. Sarcopenia is diagnosed when low muscle strength is observed in addition to low muscle quantity or quality. When low physical performance is also observed, sarcopenia is considered severe (1). The assessment of muscle quantity is well established, but muscle quality is not yet fully explored, and there is no consensus on its assessment methods (1, 2). The deposition of pathological fat in muscle tissue, known as myosteatosis, compromises the quality of skeletal muscle and appears to lead to a faster loss of strength than of muscle mass, characterizing an important parameter of loss of muscle quality (2, 3). Recent data suggests that overweight, obesity, and advanced age imply the occurrence of myosteatosis, and that its occurrence culminates in reduced functionality, muscle strength, and individual mobility (4, 5).

Type 2 Diabetes Mellitus (T2DM) is a chronic and complex metabolic disorder characterized by elevated glycemic levels due to mechanisms of increased insulin resistance (IR), associated with hyperinsulinemia and, in later stages, failure in the production and secretion of insulin by the pancreas (6). Its prevalence is recognizably associated with being overweight and obese, advanced age, and unhealthy lifestyle habits, such as sedentary behavior, high caloric intake and poor nutritional quality (6). The occurrence of T2DM can lead to chronic complications associated with micro and macroangiopathy, such as diabetic retinopathy, diabetic kidney disease, and diabetic neuropathy, in addition to being associated with cardiovascular complications (6).

Although not yet fully understood, there appears to be an association between myosteatosis and T2DM as part of the increased ectopic fat distribution. The volume of adipose infiltration in skeletal muscle is significantly higher in individuals with T2DM than in normoglycemic individuals (7). Furthermore, even in individuals without diabetes, the accumulation of fat in the trunk skeletal muscle appears to be associated with an increase in IR (8). Still, it is possible that the occurrence of myosteatosis in patients with T2DM is an independent risk factor for unfavorable outcomes, such as coronary artery calcification and acute coronary syndrome (9).

Despite the amount of studies regarding the relationship between myosteatosis and T2DM still being small, some data points to a possible connection between the two conditions, which seem to share common risk factors and present a synergistic effect in terms of morbidity and mortality (10). With this in mind, the present study sought to conduct an integrative review, with the aim of demonstrating the association between myosteatosis and T2DM or changes in glucose metabolism that contribute to the development of T2DM.

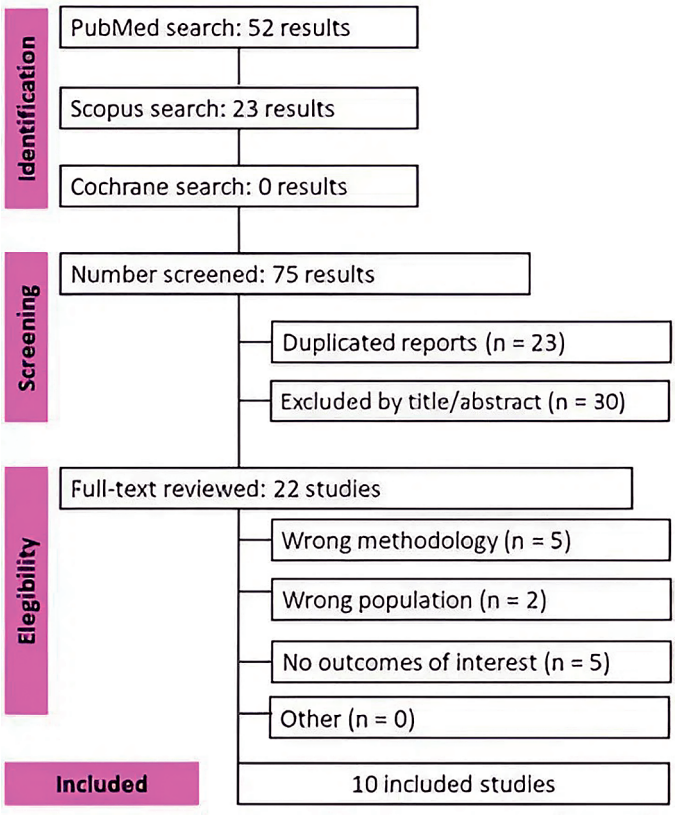

Fig. 1 Flowchart of the critical selection of articles conducted according to the recommendations of the PRISMA protocol.

MATERIALS AND METHODS

The present study is an integrative literature review, which is based on a research method grounded in the systematic synthesis of various studies and allows for the establishment of specific conclusions about a given topic (11). To guide this study with greater precision, the following guiding question was established: What is the association between myosteatosis and T2DM?

From this, the electronic research was conducted during the last three quarters of 2024. For the search, the following databases were consulted: PubMed (National Library of Medicine and National Institute of Health), Scopus, Biblioteca Virtual em Saúde (BVS), SciELO (Scientific Electronic Library Online), Cochrane Collaboration and ClinicalTrials. The inclusion criteria and filters used were articles related to the topic, studies that were not reviews or case reports and that were available in full text in the aforementioned databases. The exclusion criteria were duplicate articles, and studies on animals.

For the prospecting of the articles, the following descriptors were used: "type 2 diabetes mellitus", "non insulin dependent diabetes mellitus", "myosteatosis" and "myocellular lipid". In all databases, the combination – "(type 2 diabetes mellitus) OR (non insulin dependent diabetes mellitus) AND (myosteatosis) OR (myocellular lipid)" – was applied. In conclusion, the search was conducted by two independent reviewers and the analysis of agreement between observers was performed using the Kappa test (K) through the BioStatistics app V.1.1.0 and calculated according to the categorical method (12). The value found was K = 0.853 (almost perfect agreement).

Tab. 1 Baseline characteristics of the populations of the 10 selected studies and main findings related to glycemic status, myosteatosis and their measurement methods.

Author	Sample	ST	SP	MAP (years)	CR	MMM	Findings on glycemic status and myosteatosis
YAMAZAKI, H.; TAUCHI, S.; MACHANN, Y.; *et al. 2022*[8]	1073	Cohort study	Men and women	48	Germany and Japan	CT and MRI	AHR for incident T2DM in patients with trunk myosteatosis: 1.95 (95% CI 1.07–3.54).
KIM, E. H.; KIM, H.; LEE, M. J.; *et al. 2022*[13]	20986	Retrospective study	Men and women	54.5	South Korea	CT	Lower chances of T2DM (75% in men and 68% in women when comparing 1st and 4th quartiles) in individuals with greater muscle area with normal attenuation.
LIU, F. P.; GUO, M. J.; YANG, Q.; *et al. 2024*[9]	652	Cross-sectional Study	Men and women (with T2DM)	55.95	China	CT based on Martin's Criteria	Increased risk of coronary artery calcification in individuals with T2DM who had myosteatosis (OR = 2.381, P = 0.003).
MILJKOVIC, I.; KUIPERS, A. L.; CVEJKUS, R.; *et al. 2016*[14]	1515	Cohort study	Men	56.9	Caribbean	CT	Intermuscular fat was independently associated with a higher incidence of T2DM (OR per 1-SD increase in intermuscular fat = 1.29; 95% CI = 1.08–1.53).
MILJKOVIC, I.; CAULEY, J. A.; WANG, P. Y.; *et al. 2013*[15]	393	Cross-sectional Study	Men	74.3	United States	CT	Myosteatosis (greater infiltration of intermuscular adipose tissue in the abdominal muscles and psoas) was associated with higher glycemic levels, greater insulin resistance and hyperinsulinemia in elderly people without T2DM (in regression analyses adjusted for age, height, muscle volume, and study site, all P < 0.003).
MILJKOVIC, I.; KUIPERS, A. L.; CVEJKUS, R.; *et al. 2020*[16]	718	Cross-sectional study derived from prospective cohort	Men	64	Trinidad and Tobago	CT	Association between T2DM and liver and skeletal muscle adiposity in non-obese men, independently of visceral adiposity (in regression analyses adjusted for sociodemographic and lifestyle factors, all P < 0.05).
MILJKOVIC, I.; KUIPERS, A. L.; KAMMERER, C. M.; *et al. 2011*[17]	471	Cross-sectional study	Men and women	43	Trinidad and Tobago	CT	Markers of inflammation have been associated with myosteatosis, as well as greater insulin resistance and hypersinsulinemia – for example, higher levels of C-reactive protein correlated with lower muscle density (r = −0.10, P < 0.05), hyperinsulinemia (r = 0.12, P < 0.05), and higher HOMA-IR (r = 0.17, P < 0.01).
HUANG, Y.; YAN, J.; ZHU, H.; *et al. 2023*[18]	130	Prospective study with cohort	Men and Women	52.02	United States	MRI	Greater muscle fat infiltration (assessed by proton density fat fraction of intermuscular adipose tissue and intramuscular fat of thigh muscles) and worse muscle function (assessed by peak torque and total work of thigh muscles) in patients with T2DM compared to a control group (all with p < 0.05 in independent sample t-test).
KIEFER, L. S.; FABIAN, J.; ROS-PLESZCZ, S.; *et al. 2018*[10]	349	Retrospective study	Men and women	56	Europe*	MRI	Abdominal myosteatosis (proton density fat fraction) was significantly higher in individuals with T2DM and prediabetes compared to controls (13.1% (IQR 10.5–16.6%); 11.1% (IQR 8.9–15.0%) and 10.1% (IQR 7.5–13.3%), respectively; p < 0.001).
KIEFER, L. S.; FABIAN, J.; ROS-PLESZCZ, S.; *et al. 2021*[7]	337	Cohort study	Men and women	56	Germany	MRI	Individuals with T2DM and pre-diabetes had significantly higher amounts of intramyocellular (prediabetes: β: 0.76, 95% CI: 0.28–1.24, P = 0.002; T2DM: β: 1.56, 95% CI: 0.66–2.47, P < 0.001) and extramyocellular lipids (prediabetes: β: 1.54, 95% CI: 0.56–2.51, P = 0.002; T2DM: β: 2.15, 95% CI: 1.33–2.96, P < 0.001) than normoglycemic individuals.

Legend: AHR: Adjusted hazard ratio; CI: Confidence interval; CR: Country of Realization; CT: Computed Tomography; HOMA-IR: Homeostasis Model Assessment of Insulin Resistance; IQR: Interquartile Range; MAP: Middle Age of Patients; MMM: Measurement Method of Myosteatosis; MR: Magnetic Ressonance Imaging; OR: Odds Ratio; SD: Standard Deviation; SP: Sex of Patients; ST: Study Type; T2DM: Type 2 Diabetes Mellitus.
* Various countries around Europe.

RESULTS

A summary of the selection process can be seen below (figure 1). In total, 10 articles with various methodologies were selected for the extraction of results.

According to the selected articles (table 1), seven studies evaluated the muscle fat index through computed tomography (CT) (8, 9, 13–17), while four studies did so through magnetic resonance imaging (MRI) (7, 8, 10, 18), with one of them including both measurement methods (8). However, only one study evaluated infiltration according to Martin's criteria (attenuation of skeletal muscle (ASM) < 33 HU with body mass index (BMI) ≥ 25 kg/m² or ASM < 41 HU with BMI < 25 kg/m²) (9). Furthermore, the demographic and clinical characteristics of the patients were not considered as parameters for better evaluation and consideration of the lipid indices found. Besides, there was a great sociodemographic variability, both about the country of conduct and the general characteristics of the populations. The studies were conducted on different continents, without following a well-founded evaluation parameter for the level of lipid infiltration, including individuals without T2DM or other comorbidities in some of them.The study by Yamazaki et al. (2022) (8) explored fat distribution patterns, assessed by CT, and their relationship with the future development of T2DM. The study revealed that central fat distribution, particularly in the abdomen and muscles, was strongly associated with increased risk of diabetes, highlighting the importance of monitoring body fat in different regions to predict diabetes risk. Consistent findings were observed in the study by Kiefer et al. (2018) (10), where abdominal myosteatosis, seen on MRI, was higher in individuals with T2DM and prediabetes.

Other studies have also shown an association between myosteatosis and T2DM. Kim et al (2022) (13) found that normal muscle attenuation seen on CT reduced the chances of T2DM in a South Korean population. A cohort study with a Caribbean population showed a higher incidence of T2DM in those with myosteatosis (14). In Germany, intramyocellular and extramyocellular lipid infiltration was greater in men and women with T2DM or prediabetes than in those with normal glycemia (7). Furthermore, decreased muscle strength in patients with T2DM was associated with the presence of myosteatosis in studies that performed CT (15) and MRI (18).

The interrelationship between myosteatosis and changes in glucose metabolism is reinforced by studies that indicate that people without diabetes with greater fat deposition in skeletal muscle have lower insulin sensitivity (15, 17). A cross-sectional study with elderly Americans without T2DM demonstrated an association between myosteatosis, confirmed by CT, and greater IR and hyperinsulinemia (15). Another cross-sectional study with younger patients, developed by the same research group, showed an association between higher levels of inflammation markers, especially C-reactive protein (CRP), with adipose infiltration in the muscle, hyperinsulinemia, and IR (17).

The role of ectopic fat in the context of metabolic syndrome and T2DM can be corroborated by the findings of Mijkovic et al. (2020) (16), where there was an association between T2DM and the presence of muscle and liver adiposity in non-obese men, suggesting that myosteatosis may contribute to increased metabolic risk independently of abdominal fat. The findings of Liu et al. (2024) (9) show that in patients with T2DM the presence of myosteatosis was associated with a higher risk of coronary artery calcification, suggesting that this muscle alteration may emerge as a new risk factor for atherosclerosis in T2DM.

DISCUSSION

1. CONCEPT OF MYOSTEATOSIS

The term myosteatosis describes a condition characterized by fat infiltration in muscle tissue (4). Its main risk factors are advanced age and overweight, as both culminate in the exhaustion of the adipocytes' capacity to store lipids, so that these molecules begin to accumulate in other tissues, then being considered ectopic fat (8).

Myosteatosis can now be recognized as a clinical condition distinct from sarcopenia, originating not only from adipose tissue saturation but also from several other mechanisms. Adipogenic conversion of multipotent stem cells (through conditions such as muscle injury or increased glucocorticoid levels) and increased bone marrow adipogenesis (in situations such as prolonged bed rest, sex steroid deficiency, and altered leptin signaling) may also affect fat deposition in muscle (19).

Once considered inert, it is now known that adipose tissue has important metabolic and inflammatory capacity, and, in this way, it is understood that its accumulation in other tissues is related to several endocrinological disorders, such as decreased insulin sensitivity, hyperinsulinemia, and increased risk for the development of T2DM (4, 8).

2. MEASUREMENT METHODS

There are three types of lipid accumulation in muscle tissue that, together, are classified as myosteatosis: (a) intermuscular adipose tissue, that is, the clustering of fat below the muscle fascia and between muscle groups; (b) intramuscular adipose tissue, that is, the presence of lipid concentrates within a muscle group; and (c) intramyocellular lipids, the accumulation of fat droplets within muscle cells (2,3).

The first two forms of myosteatosis mentioned above (intermuscular adipose tissue and intramuscular adipose tissue) are the easiest to measure, with CT and MRI being the two main methods used. These exams allow for the precise and non-invasive quantification of intramuscular lipid content and the identification of specific regional patterns of fat accumulation, providing an understanding of the underlying pathophysiological mechanisms (2, 3).

Tissue density on CT can be quantified in a standardized manner using the Hounsfield unit (HU), identifying fatty infiltration by the presence of hypodense areas within the muscle. Healthy muscle presents attenuation of +30 to +150 HU, while the presence of intramyocellular lipid may present attenuation compatible with a muscle

area of low attenuation, from −29 HU to +29 HU. Intermuscular and intramuscular adipose tissue can be represented as areas of density between −30 HU and −190 HU (20). A cross-sectional analysis of 20,664 healthy adults proposed to define diagnostic cutoff points for myosteatosis, using muscle indices measured by CT at the L3 vertebra level. The ratio between the normal attenuation muscle area and the total muscle area stood out as a potentially useful index for evaluating myosteatosis, using a T-score < −2.0 as the cutoff point (21).

MRI can evaluate myosteatosis by means of the proton density fat fraction (PDFF) in T1-weighted images, suppressing the water signal. Through spectroscopy, MRI also provides measurement of intramyocellular and extramyocellular lipid contents, based on the differences in frequencies after the excitation of hydrogen nuclei (22).

CT was widely used to measure myosteatosis in the studies included in this review and is notable for its ability to visualize and quantify intermuscular and visceral fat. Some studies have used CT to assess the relationship between muscle fat and metabolic conditions (9, 13, 14). Although CT is effective in identifying hypodense areas that indicate fat, it may be less accurate in differentiating the site of fat deposition compared to MRI (2, 3). Other studies have used MRI for a detailed assessment of myosteatosis, and it is particularly useful in differentiating between intramyocellular and extramyocellular fat (7, 10, 18). Combined methods using CT and MRI have also been employed to obtain a comprehensive view of myosteatosis (8).

Quantitative ultrasound has also been studied as an imaging modality to assess myosteatosis, however, greater difficulty in standardization and the impossibility of distinguishing intramuscular and intermuscular fat are factors that hinder its implementation (3). Ultrasound was not used in any of the studies selected for this review.

3. PATHOPHYSIOLOGY OF MYOSTEATOSIS IN T2DM

Ectopic fat is found in organs such as the liver, pancreas, kidneys, heart and skeletal muscle and is associated with a pathological response in adipocyte physiology, where several genetic and environmental factors lead to inflammatory dysfunction of adipocytes and limit their ability to store fat. This leads to a redirection of lipids to peripheral tissues, leading to ectopic fat deposition (23, 24). Hypercaloric diets and hyperinsulinemia cause IR and contribute to the accumulation of fat in central organs in the pathophysiology of diabetes, such as the pancreas, liver and skeletal muscle, potentiating IR in hepatic receptors and causing impairment in pancreatic insulin secretion. This contributes to hyperglycemia and the development of T2DM (23–25).

Therefore, although not completely understood, there is a relationship between the occurrence of myosteatosis and T2DM. Individuals with T2DM have a higher amount of fat infiltrated in various muscle tissues, especially in the abdominal muscles and thigh muscles (7).

Although T2DM and myosteatosis share risk factors such as advanced age, sedentary lifestyle, and high-calorie diet, there seems to be a relationship not merely of association between the two nosological entities, but rather of causality and consequence. This is due to the fact that fat infiltration into the muscle enables the onset of a pathological triad in that tissue, composed of IR, inflammation, and contractile dysfunction (15, 16). Additionally, it has been demonstrated that greater amounts of myosteatosis are strongly associated with increased IR. The reason for this is that the accumulation of intramuscular fat impairs glucose uptake and disrupts insulin signaling. Studies using CT and MRI have consistently shown that individuals with higher myosteatosis, even when matched for visceral or total body fat, exhibit reduced muscle quality, diminished insulin sensitivity and higher Homeostatic Model Assessment of Insulin Resistance (HOMA-IR) levels. In other words, the greater the degree of myosteatosis, the higher the risk of IR and related metabolic dysfunction (15).

Another factor contributing to the occurrence of myosteatosis in patients with T2DM is the inflammatory role of adipose tissue in individuals with metabolic syndrome and obesity, particularly concerning the increased secretion of adipokines, which is directly linked to inflammation and increased IR, thereby creating a reciprocal relationship between the two conditions (1). One of the studies selected in this review demonstrated that elevated circulating inflammatory markers, including CRP, interleukin-6 (IL-6), and tumor necrosis factor-alpha (TNF-α), are closely linked to increased ectopic fat deposition in skeletal muscle, which in turn contributes to a state of persistent, low-grade inflammation. This inflammation impairs insulin receptor signaling pathways, decreasing glucose uptake by myocytes. To compensate for the reduced insulin sensitivity, pancreatic β-cells increase insulin

Fig. 2 Infographic on the relationship between myosteatosis and insulin resistance, inflammation and diabetes diabetes mellitus.

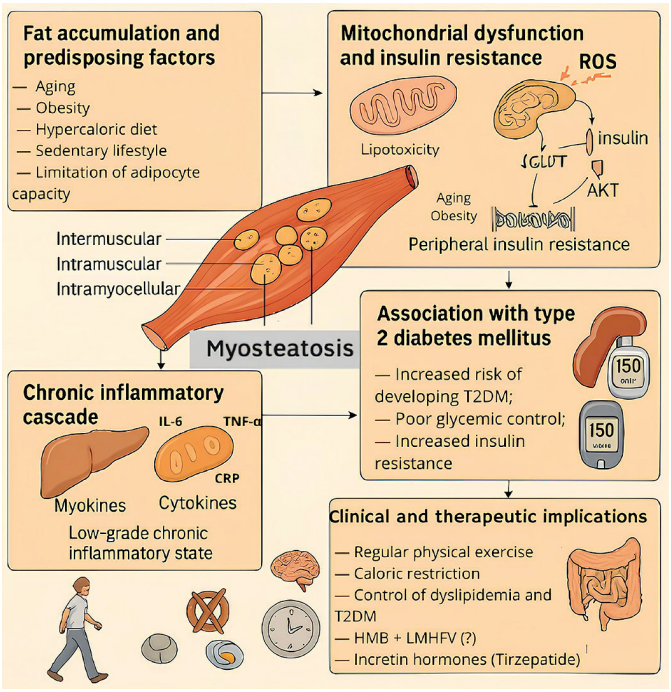

Legend: CRP: C-reactive protein; HMB: β-hydroxy β-methylbutyrate supplementation; IL-6: interleukin-6; LMHF: low-magnitude high-frequency vibration treatment; ROS: Reactive oxygen species; T2DM: Type 2 diabetes mellitus; TNF-α: tumor necrosis factor-alpha.

secretion, resulting in hyperinsulinemia. This compensatory hyperinsulinemic state further IR, thus accelerating the progression to type 2 diabetes mellitus. These findings highlight the pivotal role of inflammatory processes, inflammatory markers, and intramuscular adiposity in the pathogenesis of metabolic dysfunction and IR (17).

Figure 2 compiles the main mechanisms that link myosteatosis with IR and T2DM.

4. MYOSTEATOSIS AND INSULIN RESISTANCE IN PEOPLE WITHOUT DIABETES

The association between myosteatosis and IR in people without diabetes is mainly observed in elderly populations (15), but signs of inflammation and hyperinsulinemia are also present in younger people with larger amounts of intramuscular fat or subclinical adiposity (17).

In a cross-sectional study by Miljkovic et al. (2013) of 393 elderly men with T2DM, CT revealed that larger volumes of intermuscular fat were associated with IR, regardless of visceral fat, subcutaneous fat, or BMI (15). In a younger population, individuals without T2DM but with intramuscular fat infiltration had significantly higher levels of CRP, insulinemia, and IR, even in the absence of obesity and overt hyperglycemia (17). In a longitudinal cohort of 1,515 Afro-Caribbean men initially without T2DM, the progression of intermuscular fat was an independent predictor of T2DM development during a six-year follow-up (14). For each one-standard deviation increase in intermuscular fat, the risk of conversion to T2DM increased by 29% (OR 1.29; 95% CI: 1.08–1.53), even after adjusting for BMI and abdominal adiposity (14).

These results, consistent across different age groups and ethnic groups, indicate that myosteatosis may act as an important marker of IR and cardiometabolic risk, even in individuals with normal blood glucose levels and independently of central obesity and BMI.

5. MYOSTEATOSIS AND LIVER FAT

The accumulation of ectopic fat deposits in muscles is not only associated with T2DM and IR, but also with overall metabolic health and ectopic fat deposition at other sites. A higher proportion of good-quality muscle is strongly associated with lower risks of non-alcoholic fatty liver disease (NAFLD), as assessed by ultrasound, and liver fibrosis, as determined by the NAFLD fibrosis score and the Fibrosis-4 index. Furthermore, muscle fat content, rather than muscle mass, has been reported to be strongly and independently associated with non-alcoholic steatohepatitis (NASH) in patients with greater degrees of obesity. Collectively, these findings suggest that myosteatosis may serve as a valuable diagnostic and prognostic marker in NAFLD, a hypothesis that warrants confirmation through prospective studies (2).

6. OBSERVATIONAL STUDIES

All 10 studies selected in this review are observational, including prospective and retrospective cohorts and cross-sectional studies (Table A1). The included studies demonstrate that myosteatosis is associated with various metabolic conditions, such as obesity, IR, metabolic syndrome, cardiovascular diseases and T2DM, in addition to directly compromising muscle functionality. Greater degrees of myosteatosis was directly correlated to a decrease in muscle functionality, as shown by lower peak torque, lower total work of thigh muscles, incident mobility disability and gait speed decline in patients with myosteatosis when compared to a healthy control group (5, 18).

In studies that do not directly evaluate T2DM, evidence already suggested the harmful effect of myosteatosis. A subanalysis of the Age, Gene/Environment Susceptibility (AGES) – Reykjavik Study evaluated muscle outcomes in elderly men and women, observing that thigh myosteatosis was associated with decreased strength, slower gait and decreased survival, but no mortality relationship was observed in the same study, with calf myosteatosis. Furthermore, muscle mass loss is not uniform, and slow-twitch type I fibers are less affected than fast-twitch fibers (26).

These results reinforce that myosteatosis should be considered for metabolic and cardiovascular care, although there are still many gaps regarding the pattern of involvement and the impact on cardiovascular outcomes.

7. INTERVENTIONAL STUDIES

Therapeutic interventions to reduce myosteatosis in populations with altered glycemic status have been proposed, but not yet implemented in experimental studies. Some strategies, such as dietary changes, encouragement of physical activity, and the use of lipid-lowering medications, have shown potential to reduce intramuscular lipid accumulation and improve muscle function in individuals with myosteatosis (2–4). However, there are no studies evaluating the long-term efficacy of these interventions and their effects on the progression of associated metabolic diseases.

Despite the limitations of the currently available data regarding the impact of lifestyle on myosteatosis, there are several indications of the benefits of exercise and dietary approaches (22, 27). Consumption of a high-fat and high-fructose diet is associated with myosteatosis, especially in animal models (22, 28, 29). Implementing a calorie-restricted diet shows favorable changes in muscle composition (22, 27). The reduction of intermuscular adipose tissue has been shown to be greater when induced by exercise compared with calorie restriction alone (30). Similarly, a hypocaloric diet, when combined with aerobic exercise, may be more effective than exercise alone in reducing low-density muscle and improving glycemic status (31). A recent systematic review and meta-analysis demonstrated that exercise was able to reduce lipid infiltration in skeletal muscle and increase the muscle attenuation coefficient (32). Benefits of the combined implementation of diet and exercise are also observed in individuals with T2DM, which raises the expectation of a combined improvement in myosteatosis and dysglycemia (20, 25).

An ongoing study aims to evaluate the combined effect of low-magnitude high-frequency vibration treatment and β-hydroxy β-methylbutyrate supplementation on

myosteatosis (33), based on an animal study that showed positive results (34).

The conduct of interventional studies on myosteatosis faces significant challenges due to the absence of standardized classification criteria for this condition. The standardization of criteria is crucial considering that myosteatosis can vary widely in terms of location, severity, and functional impact, which makes it difficult to compare and generalize results between different studies. Furthermore, the variation in diagnostic methods and the definition of inclusion and exclusion criteria can lead to inconsistent and sometimes contradictory results (35–37).

In view of this, a review study highlighted the need to develop robust and universally accepted criteria for the classification of myosteatosis, in order to allow a more accurate assessment of the effectiveness of therapeutic interventions. The lack of consensus on these definitions prevents the construction of a solid evidence base, essential for the development of effective clinical guidelines and for the advancement of knowledge in this area (36).

New drugs used in the treatment of T2DM and obesity, such as tirzepatide, may perhaps provide improvement in myosteatosis, given their results in the redistribution of body fat, with a reduction in ectopic fat (38).

8. THE RELEVANCE OF ASSESSING MYOSTEATOSIS

Despite the clear association between adiposopathy and T2DM, specific data on myosteatosis and changes in glycemic status gain relevance due to the direct pathophysiological relationship with T2DM and the apparently early contractile dysfunction that myosteatosis can cause (15, 16). The loss of muscle quality due to fat infiltration generates an early reduction in strength, apparently before leading to loss of muscle quantity, so there are prospects that the assessment of myosteatosis will gain visibility in the context of the assessment of sarcopenia and clinical practice (2, 3). Data from Mijkovic et al. (2020) (16) indicate that myosteatosis is associated with T2DM independently of abdominal fat. Therefore, the assessment of ectopic fat, especially that deposited in skeletal muscle, has been shown to have an important metabolic role, so that looking only at abdominal and peripheral fat may no longer be entirely sufficient.

The improvement of assessment techniques and the standardization of diagnostic criteria bring expectations of a greater and more useful approach to myosteatosis in the clinical management of patients with T2DM or at risk of developing it.

CONCLUSIONS

Myosteatosis represents a field of research with significant implications for public health. Observational studies have enriched the understanding of this pathology with regard to associated metabolic diseases and the tests used to quantify muscle fat accumulation. However, there is no standardization among the methods of measuring myosteatosis. Furthermore, for the conduction of the studies, it is necessary to take into account the demographic variations.

Therefore, there is a need for more research to establish standardized diagnostic criteria for myosteatosis and to define the pathophysiological mechanisms of this muscle disorder in the context of T2DM and other metabolic changes. Similarly, more intervention studies will be needed that address therapeutic strategies for these patients with muscle metabolic changes in a standardized way, aiming to establish the role and effectiveness of each intervention in managing these patients.

CONFLICTS OF INTEREST

The authors declare no conflict of interest.

REFERENCES

1. Cruz-Jentoft AJ, Bahat G, Bauer J, et al. Sarcopenia: revised European consensus on definition and diagnosis. Age Ageing. 2019; 48(1): 16–31.
2. Kim HK, Kim CH. Quality Matters as Much as Quantity of Skeletal Muscle: Clinical Implications of Myosteatosis in Cardiometabolic Health. Endocrinol Metab (Seoul). 2021; 36(6): 1161–74.
3. Correa-de-Araujo R, Addison O, Miljkovic I, et al. Myosteatosis in the Context of Skeletal Muscle Function Deficit: An Interdisciplinary Workshop at the National Institute on Aging. Front Physiol. 2020; 11: 963.
4. Miljkovic I, Zmuda JM. Epidemiology of myosteatosis. Curr Opin Clin Nutr Metab Care. 2010; 13(3): 260–4.
5. Reinders I, Murphy RA, Koster A, et al. Muscle Quality and Muscle Fat Infiltration in Relation to Incident Mobility Disability and Gait Speed Decline: the Age, Gene/Environment Susceptibility-Reykjavik Study. J Gerontol A Biol Sci Med Sci. 2015; 13(8): 1030–6.
6. American Diabetes Association Professional Practice Committee; Summary of Revisions: Standards of Care in Diabetes – 2024. Diabetes Care. 2024; 47(Supplement_1): S5–S10.
7. Kiefer LS, Fabian J, Rospleszcz S, et al. Distribution patterns of intramyocellular and extramyocellular fat by magnetic resonance imaging in subjects with diabetes, prediabetes and normoglycaemic controls. Diabetes Obes Metab. 2021; 23(8): 1868–78.
8. Yamazaki H, Tauchi S, Machann J, et al. Fat Distribution Patterns and Future Type 2 Diabetes. Diabetes. 2022; 71(9): 1937–45.
9. Liu FP, Guo MJ, Yang Q, Li YY, Wang YG, Zhang M. Myosteatosis is associated with coronary artery calcification in patients with type 2 diabetes. World J Diabetes. 2024; 15(3): 429–39.
10. Kiefer LS, Fabian J, Rospleszcz S, et al. Assessment of the degree of abdominal myosteatosis by magnetic resonance imaging in subjects with diabetes, prediabetes and healthy controls from the general population. Eur J Radiol. 2018; 105: 261–8.
11. Sampaio RF, Mancini MC. Estudos de revisão sistemática: um guia para síntese criteriosa da evidência científica. Braz J Phys Ther. 2007; 11(1): 83–9.
12. Landis JR, Koch GG. The Measurement of Observer Agreement for Categorical Data. Biometrics. 1977; 33(1): 159–74.
13. Kim EH, Kim HK, Lee MJ, Bae SJ, Kim KW, Choe J. Association between type 2 diabetes and skeletal muscle quality assessed by abdominal computed tomography scan. Diabetes Metab Res Rev. 2022; 38(4): e3513.
14. Miljkovic I, Kuipers AL, Cvejkus R, et al. Myosteatosis increases with aging and is associated with incident diabetes in African ancestry men. Obesity. 2016; 24(2): 476–82.
15. Miljkovic I, Cauley JA, Wang PY, et al. Abdominal myosteatosis is independently associated with hyperinsulinemia and insulin resistance among older men without diabetes. Obesity. 2013; 21(10): 2118–25.
16. Miljkovic I, Kuipers AL, Cvejkus RK, et al. Hepatic and Skeletal Muscle Adiposity Are Associated with Diabetes Independent of Visceral Adiposity in Nonobese African-Caribbean Men. Metab Syndr Relat Disord. 2020; 18(6): 275–83.
17. Miljkovic I, Kuipers AL, Kammerer CM, et al. Markers of inflammation are heritable and associated with subcutaneous and ectopic skeletal muscle adiposity in African ancestry families. Metab Syndr Relat Disord. 2011; 9(4): 319–26.
18. Huang Y, Yan J, Zhu H, et al. Low thigh muscle strength in relation to myosteatosis in patients with type 2 diabetes mellitus. Sci Rep. 2023; 13(1): 1957.

19. Ahn H, Kim DW, Ko Y, et al. Updated systematic review and meta-analysis on diagnostic issues and the prognostic impact of myosteatosis: A new paradigm beyond sarcopenia. Ageing Res Rev. 2021; 70: 101398.
20. Kim DW, Kim KW, Ko Y, et al. Assessment of Myosteatosis on Computed Tomography by Automatic Generation of a Muscle Quality Map Using a Web-Based Toolkit: Feasibility Study. JMIR Med Inform. 2020; 8(10): e23049.
21. Kim HK, Kim KW, Kim EH, et al. Age-related changes in muscle quality and development of diagnostic cutoff points for myosteatosis in lumbar skeletal muscles measured by CT scan. Clin Nutr. 2021; 40(6): 4022–8.
22. Henin G, Loumaye A, Leclercq IA. Lanthier N. Myosteatosis: Diagnosis, pathophysiology and consequences in metabolic dysfunction-associated steatotic liver disease. JHEP Rep. 2023; 6(2): 100963.
23. Janssen, JAMJL. Overnutrition, Hyperinsulinemia and Ectopic Fat: It Is Time for A Paradigm Shift in the Management of Type 2 Diabetes. Int J Mol Sci. 2024; 25(10): 5488.
24. Snel M, Jonker JT, Schoones J, et al. Ectopic fat and insulin resistance: pathophysiology and effect of diet and lifestyle interventions. Int J Endocrinol. 2012; 2012: 983814.
25. Artasensi A, Mazzolari A, Pedretti A, Vistoli G, Fumagalli L. Obesity and Type 2 Diabetes: Adiposopathy as a Triggering Factor and Therapeutic Options. Molecules. 2023; 28(7): 3094.
26. Reinders I, Murphy RA, Brouwer IA, et al. Muscle Quality and Myosteatosis: Novel Associations with Mortality Risk: The Age, Gene/Environment Susceptibility (AGES)-Reykjavik Study. Am J Epidemiol. 2016; 183(1): 53–60.
27. Dondero K, Friedman B, Rekant J, Landers-Ramos R, Addison O. The effects of myosteatosis on skeletal muscle function in older adults. Physiol Rep. 2024; 12(9): e16042.
28. Spooner HC, Derrick SA, Maj M, et al. High-Fructose, High-Fat Diet Alters Muscle Composition and Fuel Utilization in a Juvenile Iberian Pig Model of Non-Alcoholic Fatty Liver Disease. Nutrients. 2021; 13(12): 4195.
29. Meneses MJ, Sousa-Lima I, Jarak I, Raposo JF, Alves MG, Macedo MP. Distinct impacts of fat and fructose on the liver, muscle, and adipose tissue metabolome: An integrated view. Front Endocrinol (Lausanne). 2022; 13: 898471.
30. Murphy JC, McDaniel JL, Mora K, Villareal DT, Fontana L, Weiss EP. Preferential reductions in intermuscular and visceral adipose tissue with exercise-induced weight loss compared with calorie restriction. J Appl Physiol (1985). 2012; 112(1): 79–85.
31. Prior SJ, Joseph LJ, Brandauer J, Katzel LI, Hagberg JM, Ryan AS. Reduction in midthigh low-density muscle with aerobic exercise training and weight loss impacts glucose tolerance in older men. J Clin Endocrinol Metab. 2007; 92(3): 880–6.
32. Ramírez-Vélez R, Ezzatvar Y, Izquierdo M, García-Hermoso A. Effect of exercise on myosteatosis in adults: a systematic review and meta-analysis. J Appl Physiol (1985). 2021; 130(1): 245–55.
33. Li MCM, Cheng YK, Cui C, et al. Biophysical and nutritional combination treatment for myosteatosis in patients with sarcopenia: a study protocol for single-blinded randomised controlled trial. BMJ Open. 2024; 14(1): e074858.
34. Wang J, Cui C, Chim YN, Yao H, Shi L, Xu J, et al. Vibration and β-hydroxy-β-methylbutyrate treatment suppresses intramuscular fat infiltration and adipogenic differentiation in sarcopenic mice. J Cachexia Sarcopenia Muscle. 2020; 11(2): 564–77.
35. Marcus, RL, Addison O, Kidde JP, Dibble LE, Lastayo PC. Skeletal muscle fat infiltration: impact of age, inactivity, and exercise. J Nutr Health Aging. 2010; 14(5): 362–6.
36. Mesinovic J, Fyfe JJ, Talevski J, et al. Type 2 Diabetes Mellitus and Sarcopenia as Comorbid Chronic Diseases in Older Adults: Established and Emerging Treatments and Therapies. Diabetes Metab J. 2023; 47(6): 719–42.
37. Smith, GI, Atherton, P, Reeds DN, et al. Dietary Omega-3 Fatty Acid Supplementation Increases the Rate of Muscle Protein Synthesis in Older Adults: A Randomized Controlled Trial. Am J Clin Nutr. 2011; 93(2): 402–12.
38. Cariou, B, Linge, J, Neeland IJ, et al. Effect of tirzepatide on body fat distribution pattern in people with type 2 diabetes. Diabetes Obes Metab. 2024; 26(6): 2446–55.

Prognostic Impact of Baseline Serum Creatinine in Patients with Advanced High-Grade Serous Ovarian Carcinoma Undergoing Neoadjuvant Chemotherapy

Ivan Práznovec[1,*], Jiří Špaček Jr[2], Munachiso Iheme Ndukwe[1], Denisa Pohanková[3], Eva Čermáková[3], Igor Sirák[3], Jiří Špaček[1]

ABSTRACT

Objective: To evaluate whether baseline serum creatinine is associated with survival outcomes in patients with advanced high-grade serous ovarian carcinoma undergoing neoadjuvant chemotherapy.
Methods: We retrospectively analyzed 77 patients treated between 2009 and 2018. Patients were stratified by baseline serum creatinine levels (<84 vs. ≥84 µmol/L), and survival outcomes were assessed using Kaplan-Meier analysis.
Results: No statistically significant differences in progression-free or overall survival were observed between groups. A trend toward shorter OS in the elevated creatinine group did not reach significance.
Conclusion: Baseline serum creatinine was not found to be a statistically significant prognostic marker in this cohort. These results highlight the need for adjusted analyses incorporating established prognostic factors in future research.

KEYWORDS

ovarian cancer; neoadjuvant chemotherapy; serum creatinine; prognosis

AUTHOR AFFILIATIONS

[1] Department of Obstetrics and Gynecology, Charles University, Faculty of Medicine in Hradec Králové, University Hospital Hradec Králové, Hradec Králové, Czech Republic
[2] Department of Urology, Charles University, Faculty of Medicine in Hradec Králové, University Hospital Hradec Králové, Hradec Králové, Czech Republic
[3] Department of Oncology and Radiotherapy, Charles University, Faculty of Medicine in Hradec Králové, University Hospital Hradec Králové, Hradec Králové, Czech Republic
[4] Department of Medical Biophysics, Charles University, Faculty of Medicine in Hradec Králové, University Hospital Hradec Králové, Hradec Králové, Czech Republic
* Corresponding author: Department of Obstetrics and Gynecology, Charles University, Faculty of Medicine in Hradec Králové, University Hospital Hradec Králové, Sokolská 581, 500 05 Hradec Králové, Czech Republic;
e-mail: ivan.praznovec@fnhk.cz

Received: 14 July 2025
Accepted: 15 August 2025
Published online: 6 October 2025

Acta Medica (Hradec Králové) 2025; 68(2): 45–49
https://doi.org/10.14712/18059694.2025.18

INTRODUCTION

In patients newly diagnosed with advanced high-grade serous ovarian, tubal, or peritoneal carcinoma deemed primarily inoperable, neoadjuvant chemotherapy is the standard treatment approach. Typically, 3–4 cycles of combination chemotherapy with paclitaxel and carboplatin are administered, with the exact number depending on tumor response and assessment of operability prior to planned interval debulking surgery. For patients with poorer performance status and significant comorbidities, carboplatin monotherapy may be considered, with priority given to maintaining dose intensity, such as through weekly regimens. Prior to each chemotherapy cycle, standard laboratory assessments include complete blood count, electrolytes (sodium, potassium, chloride), urea, creatinine, uric acid, bilirubin, alanine aminotransferase (ALT), and aspartate aminotransferase (AST). These parameters are crucial not only for determining the appropriate dose of carboplatin but also for monitoring potential adverse effects of systemic treatment, such as anemia, nausea, vomiting, or deterioration of renal function.

Previous studies have demonstrated that overall health status and performance status (PS) significantly influence both progression-free survival (PFS) and overall survival (OS) (1). At some institutions, the KELIM score is currently employed as a predictor of resistance to platinum-based therapies, significantly influencing PFS and OS. This score is also important for planning subsequent treatments, such as maintenance therapy with PARP inhibitors (2). Several prior studies have evaluated the prognostic significance of serum creatinine levels across various malignancies, including colorectal cancer, prostate cancer, and urothelial carcinoma (3–5).

It is therefore hypothesized that elevated serum creatinine, indicative of impaired renal function, might adversely affect the prognosis of patients with advanced high-grade serous ovarian carcinoma by necessitating dose reductions or premature discontinuation of chemotherapy. This retrospective cohort study aimed to investigate whether baseline serum creatinine levels serve as an additional prognostic parameter affecting PFS and OS in stage III and IV patients undergoing neoadjuvant chemotherapy.

METHODS

STUDY POPULATION AND DATA COLLECTION

This retrospective, single-center cohort study included 77 patients with histologically confirmed advanced high-grade serous ovarian, tubal, or peritoneal carcinoma treated between 2009 and 2018. Inclusion criteria were: completion of four cycles of neoadjuvant chemotherapy with carboplatin and paclitaxel, interval debulking surgery, and at least four cycles of postoperative chemotherapy. Patients who discontinued treatment prematurely due to disease progression, toxicity, surgery ineligibility, or incomplete data were excluded. This selection was made to ensure a homogeneous cohort with consistent treatment exposure, reducing potential confounding factors and increasing the validity of comparisons.

The primary aim was to evaluate whether baseline serum creatinine levels predict oncologic outcomes. Patients were stratified into two groups according to their baseline serum creatinine: those with levels below 84 μmol/L and those with levels equal to or above 84 μmol/L, in accordance with the local reference range. The primary endpoints were progression-free survival (PFS) and overall survival (OS), measured from the date of diagnosis to the date of radiologically confirmed progression or death, respectively.

Baseline serum creatinine levels were obtained from hospital electronic medical records (NIS, Medicalc) at the time of the first neoadjuvant chemotherapy cycle. Diagnosis date, date of disease progression (based on CT imaging), and date of death were retrieved to assess PFS and OS.

Patient characteristics such as age, menopausal status, hormone replacement therapy (HRT) use, parity, CA-125 level, BMI, FIGO stage (III vs. IV), and postoperative surgical residuum were also collected. FIGO staging and residual tumor status were confirmed from surgical and pathological reports. Optimal cytoreduction was defined as R0 (no macroscopic residual tumor) or R1 (macroscopic residual tumor <1 cm); suboptimal cytoreduction was defined as R2 (macroscopic residual tumor ≥1 cm).

Statistical analyses were performed using NCSS 2023 software (NCSS, LLC., Kaysville, Utah, USA). Descriptive statistics were presented as absolute and relative frequencies for categorical variables, and means or medians with range for continuous variables. Kaplan-Meier survival analysis and log-rank tests were used to evaluate PFS and OS. Differences in categorical variables (FIGO stage, surgical residuum) between creatinine groups were evaluated using Fisher's exact test. Significance was set at $\alpha = 0.05$. A post hoc power analysis was conducted using a two-sided comparison of means based on the observed 6-month difference in overall survival between groups. The standard deviation (SD = 4.7 months) was calculated directly from the distribution of overall survival in the study cohort.

This retrospective study was conducted in accordance with the Declaration of Helsinki and was approved by the Ethics Committee of the University Hospital Hradec Králové. The requirement for individual informed consent was waived due to the retrospective design and anonymized data handling.

SERUM CREATININE ASSESSMENT

Measurement of serum creatinine (S-crea) is part of routine daily clinical practice. It is a cost-effective and commonly used method, although its interpretation can be challenging. Clinicians recognize that serum creatinine levels are influenced by muscle catabolism and can thus be either decreased or increased under various conditions such as anorexia, obesity, or after physical exertion. Identical serum creatinine values can correspond differently to glomerular filtration rate (GFR), which depends on gender, age, height, weight, and ethnicity (6). Physiologically

and pathophysiologically, creatinine secretion occurs in the renal tubules, explaining why creatinine clearance often overestimates the actual GFR. This overestimation can be unpredictable and may fluctuate over time in individual patients (7). Serum creatinine levels are also affected by patient nutrition, particularly a protein-rich diet. Nutritional enteral support with high protein content, which many patients receive, should also be considered (8). Additionally, literature describes extrarenal creatinine clearance by intestinal bacteria, contributing to reduced excretion, especially in patients with chronic kidney disease (9). Establishing correct reference intervals is difficult due to variations influenced by age, gender, and ethnicity. These variations were addressed by Pottel et al., who established age – and gender-specific intervals, mainly for the Caucasian population. Serum creatinine physiologically declines after birth, subsequently increases linearly with age, and remains relatively constant between 20–70 years of age in healthy individuals. In women over 70 years, serum creatinine levels physiologically increase (10). Tracking serum creatinine trends over time in individuals, particularly older adults, is more advantageous than relying solely on a single measurement, although even one measurement can indicate potential renal dysfunction (11).

Serum creatinine was measured using a COBAS 8000 analyzer (Roche, Mannheim, Germany) in the certified laboratory at University Hospital Hradec Králové. The enzymatic method employed involves converting creatinine to glycine, formaldehyde, and hydrogen peroxide through enzymes creatininase, creatinase, and sarcosine oxidase. Released hydrogen peroxide reacts catalytically with peroxidase, 4-aminophenazone, and HTIB to form a quinoneimine chromogen. The color intensity of this chromogen is directly proportional to the creatinine concentration in the reaction mixture. The local laboratory reference range for women is 45–84 µmol/L.

RESULTS

DESCRIPTIVE STATISTICS

Baseline characteristics stratified by serum creatinine are presented in Table 1. The median age was 64 years (range 31–87) in the normal creatinine group and 66 years (range 40–85) in the elevated group, with mean ages of 63.8 (SD 9.2) and 65.0 (SD 8.8), respectively. Postmenopausal status predominated in both groups (95% vs. 94%). Hormone replacement therapy use was reported in 7% of the normal group and 6% of the elevated group.

The median baseline CA-125 level was 1043 kU/L in the normal creatinine group and 1132 kU/L in the elevated group. Median BMI was comparable (25.6 vs. 26.0 kg/m²). Suboptimal cytoreduction (R2) occurred in 31% of patients with normal creatinine versus 78% in the elevated group. R0 resection was achieved in 49% and 22%, respectively, while no R1 resections occurred in the elevated creatinine group.

FIGO stage III disease was present in 80% of the normal creatinine group and 83% of the elevated group. Stage IV was found in 20% and 17%, respectively. Smoking prevalence was 7% versus 11%, arterial hypertension was noted in 22% versus 28%, and diabetes mellitus in 14% versus 22%, for the normal and elevated creatinine groups, respectively.

GROUP STRATIFICATION AND OUTCOMES

Patients were divided into two groups based on baseline serum creatinine (S-crea): those with levels <84 µmol/L (normal range) and those with levels ≥84 µmol/L. There were 59 patients (76.62%) in the normal S-crea group and 18 patients (23.38%) in the elevated S-crea group. Among the patients with normal S-crea, 80% had stage III and 20% had stage IV; among those with elevated S-crea, 83% had stage III and 17% had stage IV. There was no significant

Tab. 1 Descriptive parameters and their frequencies in the study cohort.

Parameter	Normal S-crea <84 µmol/L (n=59)	Elevated S-crea ≥84 µmol/L (n=18)
Age in years	Median 64 (range 31–87) Mean 63.8 (SD 9.2)	Median 66 (range 40–85) 65 (SD 8.8)
Menopausal status	Premenopausal: 3 (5%) Postmenopausal: 56 (95%)	Premenopausal: 1 (6%) Postmenopausal: 17 (94%)
HRT use	4 (7%)	1 (6%)
CA-125 (kU/L)	Median 1043	Median 1132
BMI (kg/m²)	Median 25.6	Median 26.0
Postoperative residuum	R0: 29 (49%), R1: 12 (20%), R2: 18 (31%)	R0: 4 (22%), R1: 0 (0%), R2: 14 (78%)
FIGO stage	III: 47 (80%), IV: 12 (20%)	III: 15 (83%), IV: 3 (17%)
Smoking	4 (7%)	2 (11%)
Arterial Hypertension	13 (22%)	5 (28%)
Diabetes mellitus	8 (14%)	4 (22%)

difference in FIGO stage distribution between the two creatinine groups (p = 0.462).

In terms of surgical outcomes, 69.5% of patients in the normal S-crea group had R0/R1 resection compared to 44.4% in the elevated S-crea group. Conversely, 30.5% of the normal S-crea group and 55.6% of the elevated group had R2 resection. This difference was not statistically significant (p = 0.120), although a trend toward worse surgical outcome in the elevated creatinine group was noted.

Regarding survival outcomes, there was no statistically significant difference in PFS between the two groups. The median PFS was 14 months (95% CI: 13–17) in the normal creatinine group compared to 12 months (95% CI: 9–15) in the elevated creatinine group (p = 0.951). Similarly, OS was not significantly different, although numerically shorter in the elevated creatinine group. The median OS was 31 months (95% CI: 22–41) in the normal group compared to 25 months (95% CI: 14–32) in the elevated group (p = 0.316). Figure 1 and Figure 2 presents the PFS and OS, respectively. A post hoc power analysis based on the observed OS difference (31 vs. 25 months) and the calculated SD of 4.7 months indicated a statistical power of 99.7%, suggesting a very low probability of Type II error.

DISCUSSION

This retrospective single-center study investigated whether baseline serum creatinine levels have prognostic value in patients with advanced high-grade serous ovarian carcinoma undergoing neoadjuvant chemotherapy. Although the differences did not reach statistical significance, patients with elevated creatinine levels had numerically shorter progression-free and overall survival, as well as a higher rate of suboptimal cytoreduction (R2). These findings suggest that serum creatinine may reflect underlying physiological vulnerability or treatment tolerance, and therefore may hold potential as a supportive prognostic marker.

Our data showed that patients with elevated serum creatinine were less likely to achieve optimal cytoreduction. While 69.5 percent of patients with normal creatinine levels underwent R0 or R1 resection, only 44.4 percent in the elevated creatinine group did so. Conversely, the rate of suboptimal cytoreduction (R2) was higher in the elevated creatinine group. Although the difference was not statistically significant, this trend may indicate impaired surgical outcomes in patients with compromised baseline renal function. A similar trend was observed in overall survival, where patients with elevated creatinine had a median OS of 25 months compared to 31 months in the normal group. These associations, while not conclusive, are clinically relevant and warrant further investigation.

In recent years, interest has grown in identifying pre-treatment laboratory markers that reflect systemic inflammation, nutritional status, or comorbidity burden. Studies have shown that markers such as IL-37 and plasma fibrinogen may outperform traditional tumor markers like CA-125 in prognosticating advanced epithelial ovarian cancer (12, 13). These data support the notion that simple blood-based biomarkers can contribute to risk stratification. Nutritional status is also known to impact outcomes. Low albumin levels, for example, have been linked to delayed wound healing, which in turn may postpone adjuvant chemotherapy and negatively affect prognosis (14). Creatinine levels, although primarily associated with renal function, are also influenced by muscle mass and protein intake, both of which relate closely to nutritional status and frailty. Emerging evidence also points to the role of physical activity in improving cancer outcomes. Kanbay et al. demonstrated that exercise reduces inflammation and oxidative stress while enhancing cardiovascular function and immune competence, all of which are likely to contribute to improved tolerance of systemic treatment and potentially better survival (16).

This study has several limitations, primarily its retrospective design, which restricts control over confounding factors. BRCA mutation status was unavailable for most patients, as routine testing was only implemented later in the study period. Although the cohort size was modest, a post hoc power analysis based on patient-level survival data (α = 0.05, pooled SD = 4.7 months, n = 59 vs. 18) demonstrated approximately 99.7% power to detect the observed 6-month OS difference. This suggests that the lack of statistical significance is unlikely to be due to insufficient sample size. However, given the inherent limitations of retrospective analyses, these findings should be interpreted with caution and validated in prospective studies.

In light of our findings, serum creatinine may not serve as a standalone prognostic factor, but rather as a surrogate

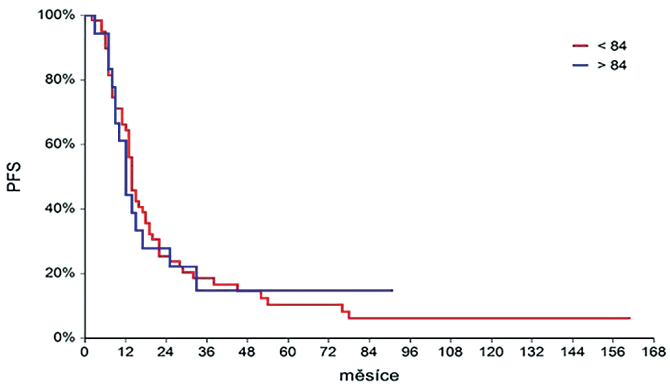

Fig. 1 Progression-free survival (PFS).

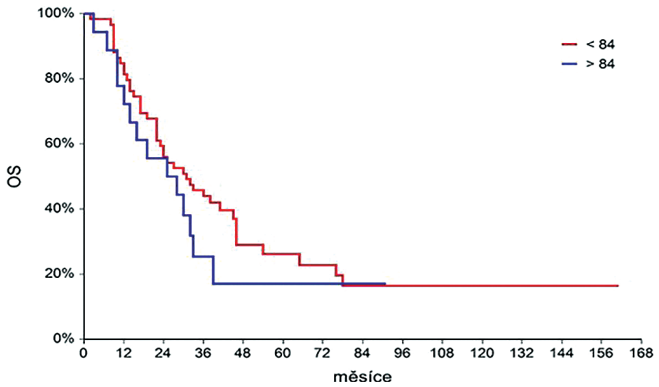

Fig. 2 Overall survival (OS).

for broader patient-related variables such as comorbidities, nutritional state, and functional reserve. The observed trends highlight the need for prospective studies to determine whether baseline creatinine, in combination with other biomarkers, could reliably support clinical decision-making in this population.

CONCLUSIONS

Our retrospective study found a non-significant trend toward shorter survival in patients with elevated baseline serum creatinine undergoing treatment for advanced ovarian cancer. While not sufficient to establish serum creatinine as an independent prognostic factor, these findings warrant further prospective evaluation of its potential role in combination with other clinical and biochemical markers.

REFERENCES

1. Carey MS, Bacon M, Tu D, Butler L, Bezjak A, Stuart GC. The prognostic effects of performance status and quality of life scores on progression-free survival and overall survival in advanced ovarian cancer. Gynecol Oncol. 2008 Jan; 108(1): 100–5.
2. Piedimonte S, Kim R, Bernardini MQ, et al. Validation of the KELIM score as a predictor of response to neoadjuvant treatment in patients with advanced high grade serous ovarian cancer. Gynecol Oncol. 2022 Dec; 167(3): 417–22.
3. Giessen-Jung C, Nagel D, Glas M, et al. Preoperative serum markers for individual patient prognosis in stage I–III colon cancer. Tumour Biol. 2015 Sep; 36(10): 7897–906.
4. Tollefson MK, Boorjian SA, Gettman MT, Rangel LJ, Bergstralh EJ, Karnes RJ. Preoperative estimated glomerular filtration rate predicts overall mortality in patients undergoing radical prostatectomy. Urol Oncol. 2013 Nov; 31(8): 1483–8.
5. Kim M, Moon KC, Choi WS, et al. Prognostic value of systemic inflammatory responses in patients with upper urinary tract urothelial carcinoma. World J Urol. 2015 Oct; 33(10): 1439–57.
6. Perrone RD, Madias NE, Levey AS. Serum creatinine as an index of renal function: new insights into old concepts. Clin Chem. 1992 Oct; 38(10): 1933–53.
7. Bauer JH, Brooks CS, Burch RN. Clinical appraisal of creatinine clearance as a measurement of glomerular filtration rate. Am J Kidney Dis. 1982 Nov; 2(3): 337–46.
8. King AJ, Levey AS. Dietary protein and renal function. J Am Soc Nephrol. 1993 May; 3(11): 1723–37.
9. Mitch WE, Walser M. A proposed mechanism for reduced creatinine excretion in severe chronic renal failure. Nephron. 1978; 21(5): 248–54.
10. Pottel H, Vrydags N, Mahieu B, Vandewynckele E, Croes K, Martens F. Establishing age/sex related serum creatinine reference intervals from hospital laboratory data based on different statistical methods. Clin Chim Acta. 2008 Oct; 396(1–2): 49–55.
11. Sottas PE, Kapke GF, Leroux JM. Adaptive Bayesian approach to clinical trial renal impairment biomarker signal from urea and creatinine. Int J Biol Sci. 2013; 9(2): 156–63.
12. Huo J, Hu J, Liu G, Cui Y, Ju Y. Elevated serum interleukin-37 level is a predictive biomarker of poor prognosis in epithelial ovarian cancer patients. Arch Gynecol Obstet. 2017 Feb; 295(2): 459–65.
13. Luo Y, Kim HS, Kim M, Lee M, Song YS. Elevated plasma fibrinogen levels and prognosis of epithelial ovarian cancer: a cohort study and meta-analysis. J Gynecol Oncol. 2017 May; 28(3): e36.
14. Mendivil AA, Rettenmaier MA, Abaid LN, Brown JV 3rd, Mori KM, Goldstein BH. The impact of total parenteral nutrition on postoperative recovery in patients treated for advanced stage ovarian cancer. Arch Gynecol Obstet. 2017 Feb; 295(2): 439–44.
15. Aapro M, Beguin Y, Bokemeyer C, Dicato M, Gascón P, Glaspy J, Hofmann A, Link H, Littlewood T, Ludwig H, Österborg A, Pronzato P, Santini V, Schrijvers D, Stauder R, Jordan K, Herrstedt J. ESMO Guidelines Committee. Management of anaemia and iron deficiency in patients with cancer: ESMO Clinical Practice Guidelines. Ann Oncol. 2018 Oct 1; 29(Suppl 4): iv96–iv110. Erratum in: Ann Oncol. 2018 Oct 1; 29(Suppl 4): iv271.
16. Kanbay M, Copur S, Yildiz AB, Tanriover C, Mallamaci F, Zoccali C. Physical exercise in kidney disease: A commonly undervalued treatment modality. Eur J Clin Invest. 2024 Feb; 54(2): e14105.

Comparative Analysis of Immaturity CD Markers Expression between Pediatric and Adult Acute Lymphoblastic Leukemia: Insights and Implications for Diagnostic and Therapeutic Strategies

Ihsan Mardan Al-Badran[1,*], Ahmed Mardan Al-Badran[2]

ABSTRACT

Objective: The objective of this study is to assess the expression levels of different immaturity CD markers in diverse subtypes of Acute Lymphoblastic Leukemia (ALL) among children and adults, and determine any statistically significant variations in marker expression between these two groups.

Methods: This dataset included CD marker expressions (CD34, HLA-DR, TdT, and CD38) for 130 ALL patients (51 pediatric B-ALL, 16 pediatric T-ALL, 44 adult B-ALL, and 19 adult T-ALL patients). The Shapiro-Wilk test analysis was conducted to check for normality distribution in all data points before proceeding with the statistical analysis test. As a result for each marker within these subtypes, descriptive statistics were calculated. Independent samples t-tests were initially conducted to compare mean expression levels of CD markers between groups. Moreover, since non-normal distributions are likely to occur, Mann-Whitney U tests were used for Pediatric T-ALL and Adult T-ALL.

Results: Descriptive analysis indicated variability in CD marker expression levels among the different subtypes of ALL. Both t-tests and Mann-Whitney U tests revealed statistically significant differences ($p < 0.05$) in the expression levels of CD markers between pediatric and adult groups, or between B-ALL and T-ALL groups.

Conclusion: Significant differences have been identified using different analysis methods across the studied groups. The investigation analyzes the expression levels of CD34, HLA-DR CD38, and TdT within pediatric B-ALL patients and pediatric T-ALL patients along with adult B-ALL patients and adult T-ALL patients. The patterns need appreciation because they might reveal biological differences at their base which influence disease development and both treatment results and patient survival outcomes.

KEYWORDS

acute lymphoblastic leukemia; CD markers; statistical analysis; Mann-Whitney U test; data imputation

AUTHOR AFFILIATIONS

[1] Department of Pathology and Forensic Medicine, Al-Zahraa College of Medicine, University of Basrah, Basrah, Iraq
[2] Department of Radiation Oncology, Basra Oncology Center, Basra Directorate of Health, Basrah, Iraq
* Corresponding author: Department of Pathology and Forensic Medicine, Al-Zahraa College of Medicine, University of Basrah, Basrah, Iraq; e-mail: ihsanmardan@uobasrah.edu.iq

Received: 24 December 2024
Accepted: 25 June 2025
Published online: 6 October 2025

Acta Medica (Hradec Králové) 2025; 68(2): 50–57
https://doi.org/10.14712/18059694.2025.19

INTRODUCTION

Acute Lymphoblastic Leukemia (ALL) develops as lymphoid malegnancy that presents as uncontrolled lymphoid precursor cell growth which leads to the buildup of unmatured lymphocytes throughout the bone marrow and outside the marrow sites (1). The occurrence of acute lymphoblastic leukemia represents the highest frequency among pediatric malignancies such that this disease type affects both children and adults but demonstrates more aggressive behavior among elderly patients (2). The research targets lymphoid leukemias exclusively despite the possibility for hematological cancers to develop from myeloid and lymphoid origins.

The classification of ALL includes two primary types defined by their cellular origins between B-cell and T-cell lymphoid cells. Different All subtypes require unique diagnostic methods and personalized treatment strategies because they present separate biological characteristics as well as prognostic features (3). Flow cytometry uses a cluster of differentiation markers to analyze cell surface and cytoplasmic proteins through a process that diagnoses and classifies lymphoid leukemias effectively (4). The cell markers defining B-lineage ALL include CD10 and CD19 in combination with CD20 while T-lineage ALL shows positive results for markers CD2 and CD3 and CD7. The obtained immunophenotypic information about leukemia delivers vital biological information for designing the treatment strategy.

Therefore, Adult patients who have lymphoid leukemias show worse medical results compared to pediatric patients despite recent treatment innovations with targeted treatments and immunotherapies (5). The observation highlights the need to analyze immune and molecular patterns that exist between pediatric and adult ALL along with B-ALL and T-ALL subtypes. The research design in this study aims to discover systematic expression differences of immaturity markers which include CD34, CD38, HLA-DR, and TdT rather than asserting that B-ALL and T-ALL are Equivalent groups. Research analysis between these profiles allows us to create more precise diagnostic methods and better subgroup the lymphoid leukemia category while discovering new biomarkers that enhance both treatment predictions and customized therapeutic plans (6).

This study analyzes the distribution of immature CD markers (CD34, CD38, HLA-DR, TdT) which appear in various leukemia and lymphoma diagnoses for pediatric and adult patients. Our goal after examining these markers will be to make decisions about diagnostic criteria along with refining subclassification protocols. Targeted therapy can become more achievable with the adoption of an improved diagnostic system that benefits facilities that lack advanced immunophenotyping tools. The objective of this study is to identify valuable details for risk assessment and treatment strategy development instead of tracking treatment outcomes between B-ALL and T-ALL patient groups.

The objective of this study differed from diagnostic category redefinition since B-ALL and T-ALL markers already distinguish between these subtypes. The research investigated how immaturity-associated markers (CD34, TdT) displayed their expression patterns both between and within subtypes in children versus adult populations because these findings could help improve treatment strategies and prognostic forecasting and minimal residual disease (MRD) testing methods particularly in locations where advanced tests are scarce.

PREVIOUS STUDIES

Acute Lymphoblastic Leukemia CD markers can be used as diagnostic tools for diagnosis, prognosis, and therapy, Porwit et al. (2019) carried out a detailed study on the immunophenotypic characteristics of pediatric ALL stressing the importance of CD10, CD19, and CD34 in B-ALL; while T-ALL is characterized by CD2, CD3, and CD7 (7). They also found that bad outcome was associated with poor clinical prognostication significance of high expression of CD34. Similarly, Emmirc et al. (2022) focused on adult ALL and characterized distinctive patterns of expression of different subtypes using different CD markers such as B-lymphoid or T-lymphoid origin. They stressed the fact that fluctuation in marker intensity might lead to personalized treatment options based on changing levels of protein

Tab. 1 Previous Related Studies.

Method	Results	Limitations	Authors
Immunophenotypic Characteristics of Pediatric Acute Lymphoblastic Leukemia Flow cytometric examination of CD markers in children suffering from ALL	CD10, CD19, and CD34 were recognized as significant markers in B-ALL while those of T-ALL included CD2, CD3, CD7 and CD34	More Samples need to be investigated	(10)
Immunophenotypic Analysis of Adult Acute Lymphoblastic Leukemia undergoing flow cytometry immunophenotyping	B-ALL and T-ALL subtypes had different levels of expression for the same CD markers, showing that the variations in the expression are large. Included only adult patients	Small sample size	(11)
Comparative Analysis of CD Marker Expression in Pediatric and Adult ALL Patients Differentiation between pediatric and adult ALL is made by studying the variation between their corresponding CD marker profiles using flow cytometry	The differences between pediatric and adult leukemias were obvious as well as those between B-cell acute lymphocytic leukemia (B-ALL) and T-cell acute lymphocytic leukemia (T-ALL)	No clinical outcome data was provided for these cases that did not relate CD marker profile to pathogenesis which may have required a larger sample size	(12)

expression (8). In their recent study Mahapatra et al., 2019 employed flow cytometry to investigate a broad panel of previously established and newly published markers expressed in ALL patients both children and adults revealing differences within age groups and between subtypes (9). Despite this progress however, more comprehensive studies are needed to fully understand the biological and clinical relevance of such antigens, especially during a period wherein novel targeted therapies including monoclonal antibodies are being developed for use against them in this disease. Table 1 shows previous related studies.

METHOD

STUDY DESIGN AND PATIENT POPULATION

The study used retrospective observational methods to measure CD markers associated with immaturity in the blood cells of both pediatric and adult patients with ALL. This research analyzed 130 patients with newly diagnosed ALL who were subdivided based on their age together with their immunophenotypic subtype.

- Pediatric B-ALL: 51 patients
- Pediatric T-ALL: 16 patients
- Adult B-ALL: 44 patients
- Adult T-ALL: 19 patients

Laboratory testing was conducted according to EGIL criteria and determined B-lineage through CD19/CD79a marker analysis or T-lineage through CD3/CD7/CD2 marker testing. Patients who had biphenotypic or mixed phenotype ALL were excluded from the study.Moreover, the main samples used in this study came from bone marrow aspirates which patients provided at their diagnosis stage. The analysis used peripheral blood samples when bone marrow aspiration proved unavailable while meeting the requirements of WHO recommendations for flow cytometric immunophenotyping and having blast cells at or above 20% in the samples. Moreover, a retrospective descriptive study designed to include 130 pediatric (aged ≤ 18 years) and adult patients (>18 years) with newly diagnosed ALL who were admitted to the hematology unit at Medical City Hospital in Baghdad for the period between July 2022 and July 2024.

DIAGNOSTIC CRITERIA AND CLASSIFICATION

All patients have data for clinical parameters, complete blood pictures, bone marrow examination, and immunophenotypes. The diagnosis was based on cytomorphology of the peripheral blood and/or bone marrow aspirate samples by an expert hematopathologist in the laboratories of Medical City Hospital. Fundamental types of B-ALL and T-ALL diagnosis followed both the WHO classification guidelines from 2017 and the recommendations of EGIL.

FLOW CYTOMETRY AND DATA ACQUISITION

This study performed leukemic blast marker analysis on BD FACSCanto II flow cytometer (BD Biosciences) located in San Jose, CA. Scientists employed monoclonal antibodies attached to fluorochromes to detect different cell markers during their analysis. Table 2 shows monoclonal antibodies used in this study for Flow Cytometric Immunophenotyping.

Tab. 2 Monoclonal Antibodies.

Marker	Fluorochrome	Clone	Manufacturer
CD10	FITC	HI10a	BD Biosciences
CD19	PE	HIB19	BD Biosciences
CD34	APC	581	BD Biosciences
HLA-DR	PerCP	L243	BD Biosciences
TdT	FITC	HT-6	Beckman Coulter
CD38	PE-Cy7	HIT2	BD Biosciences
CD3	APC	UCHT1	BD Biosciences
CD2	PerCP	RPA-2.10	BD Biosciences
CD7	FITC	M-T701	BD Biosciences

The study used BD Biosciences and Beckman Coulter as its source for antibody procurement. Before cytometry analysis, the sample preparation process involved washing bone marrow or peripheral blood while lysing RBCs before suspending the solution in PBS reagent.

DATA ANALYSIS SOFTWARE AND NORMALITY TESTING

BD FACSDiva™ v8.0 software enabled data acquisition while also preprocessing the data in a manner that enabled the use of gating to remove debris and doublets and therefore separate the blast population. The software program BD FACSDiva™ v8.0 registered Median Fluorescence Intensity (MFI) values for each population as part of the data acquisition process. The researchers transferred MFI values to ensure statistical analysis through IBM SPSS Statistics version 23.

The Shapiro-Wilk test checked for normality distribution in all data points before running statistical procedures as shown in Table 3. The Shapiro-Wilk test served to determine between using parametric or non-parametric tests during comparisons. Results from normality testing

Tab. 3 Shapiro-Wilk Test for Normality of CD Marker Expression.

CD Marker	Pediatric B-ALL (n = 51)	Pediatric T-ALL (n = 16)	Adult B-ALL (n = 44)	Adult T-ALL (n = 19)
CD34	p-value = 0.128	p-value = 0.041	p-value = 0.212	p-value = 0.002
HLA-DR	p-value = 0.093	p-value = 0.004	p-value = 0.452	p-value = 0.031
TdT	p-value = 0.254	p-value = 0.021	p-value = 0.376	p-value = 0.023
CD38	p-value = 0.317	p-value = 0.065	p-value = 0.152	p-value = 0.019

methods appear in the following table regarding group and CD marker assessment.

COMPARATIVE AND CORRELATION ANALYSIS

Parametric Tests (Independent t-tests) were conducted in this study due to their design that can handle normally distributed data for Pediatric B-ALL and Adult B-ALL. Moreover, Non-parametric Tests (Mann-Whitney U tests) were conducted for data that did not follow a normal distribution which are Pediatric T-ALL and Adult T-ALL.

The following comparisons were made:

- Pediatric B-ALL along with Adult B-ALL
- Pediatric T-ALL along with Adult T-ALL
- Pediatric B-ALL along with. Pediatric T-ALL
- Adult B-ALL along with Adult T-ALL

Furthermore, Pearson correlation was used to study relationships in marker expression across subtypes. The significance threshold $p < 0.05$ was adopted for all statistical tests.

DATA PREPROCESSING AND MISSING VALUE IMPUTATION

Missing values (<5%) were replaced using mean substitution in the Adult B-ALL and Adult T-ALL groups under the assumption of random occurrence. Expression data were normalized to reduce scale-based variances that could influence group comparisons.

ETHICAL CONSIDERATIONS

The study protocol was examined and approved by the Institutional Review Board or Ethics Committee. Written informed consent was obtained from the guardians in the case of minors and from adult patients, following procedures in line with the Declaration of Helsinki.

PRACTICAL IMPLICATIONS

Powerful diagnostic and prognostic details can be extracted from simple immunophenotypic assays using the CD34, HLA-DR, TdT, and CD38 marker combinations, particularly in a resource-constrained setting. Therefore, this enables the classification of B-ALL and T-ALL subtypes by cytometry experts, thus assisting in diagnostic and management decisions in an environment with limited laboratory services.

RESULTS

CD marker descriptive statistics across the four groups such as Pediatric B-ALL, Pediatric T-ALL, Adult B-ALL, and Adult T-ALL showed variability in marker expression. Table 4 and Figure 1 show Key findings from the descriptive statistics.

Table 4 summarizes the mean and standard deviation (SD) values of some main CD markers among different patient groups. CD34 has higher average expressions in Pediatric B-ALL and Adult B-ALL compared to their counterparts of T-All. Such patterns resemble those of HLA-DR and TdT. To evaluate and conduct a more comparative analysis, independent samples t-tests were performed. Table 5 and Figure 2 show the initial comparison using independent samples t-tests.

These p-values imply that no significant changes ($p < 0.05$) in the CD34, HLA-DR, and TdT expression levels were found in data of Pediatric B-ALL compared to Adult B-ALL or between Pediatric T-ALL and Adult T-ALL. However, some markers showed marginal significance when comparing Pediatric B-ALL vs Pediatric T-ALL. Therefore, since non-normal distributions are likely to occur, Mann-Whitney U tests were used, Table 6 and Figure 3 show the results from Mann-Whitney U tests.

The t-test results indicate that most of the Mann-Whitney U tests for the comparison between groups did not reach statistical significance for CD marker expression levels except for some marginal significance in the case of Pediatric B-ALL vs. Pediatric T-ALL comparisons.

Moreover, there are other categories such as Pediatric B-ALL, Pediatric T-ALL, Adult B-ALL, and Adult T-ALL in which a correlation matrix of CD markers can shed light on relationships between the expression levels of these markers. It is noted that there exists a higher positive correlation ($r = 0.981$) between Pediatric B-ALL and Adult B-ALL indicating great similarity in the expression of CD markers among these two groups suggesting that immunophenotypic profiles concerning B-cell ALL remain consistent not only within pediatric but also across adult patients. Similarly, a high positive correlation ($r = 0.892$) between Pediatric T-ALL and Adult T-ALL indicates the closeness in their patterns of CD marker expression across different age ranges for individuals diagnosed with this disease type. On the other hand, however, there was a very low correlation ($r = 0.013$) between Pediatric B-ALL and Pediatric T-ALL which points out to differences between

Tab. 4 Descriptive Statistics of CD Marker Expression in ALL Patients (Values Expressed in Median Fluorescence Intensity [MFI] Units).

CD Marker	Pediatric B-ALL (n = 51)	Pediatric T-ALL (n = 16)	Adult B-ALL (n = 44)	Adult T-ALL (n = 19)
CD34	Mean = 42, SD = 17.88, IQR = 30–54	Mean = 7, SD = 5.48, IQR = 4–9	Mean = 36, SD = 16.97, IQR = 25–47	Mean = 8, SD = 6.36, IQR = 5–10
HLA-DR	Mean = 51, SD = 17.88, IQR = 38–64	Mean = 1, SD = 5.48, IQR = 0–2	Mean = 44, SD = 16.97, IQR = 33–56	Mean = 6, SD = 6.36, IQR = 3–8
TdT	Mean = 42, SD = 17.88, IQR = 30–55	Mean = 10, SD = 5.48, IQR = 7–13	Mean = 41, SD = 16.97, IQR = 30–53	Mean = 16, SD = 6.36, IQR = 12–19
CD38	Mean = 60, SD = 15.5, IQR = 50–70	Mean = 28, SD = 10.2, IQR = 20–35	Mean = 55, SD = 14.6, IQR = 44–66	Mean = 25, SD = 11.4, IQR = 18–33

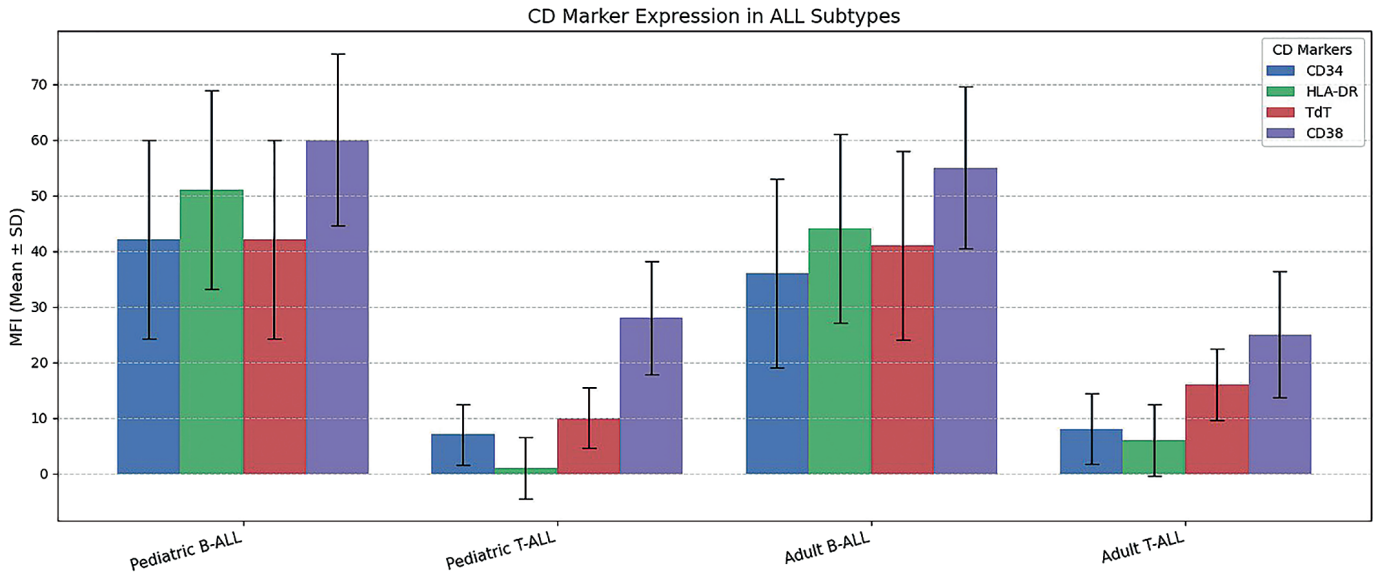

Fig. 1 Mean ± SD for All CD Markers.

Tab. 5 Independent Samples T-tests for CD Marker Expression Between Patient Groups.

CD Marker	p-value (Pediatric B-ALL vs. Adult B-ALL)	p-value (Pediatric T-ALL vs. Adult T-ALL)	p-value (Pediatric B-ALL vs. Pediatric T-ALL)	p-value (Adult B-ALL vs. Adult T-ALL)
CD34	0.456	0.789	0.034	0.067
HLA-DR	0.112	0.543	0.002	0.145
TdT	0.678	0.123	0.021	0.054
CD38	0.200	0.045	0.035	0.090

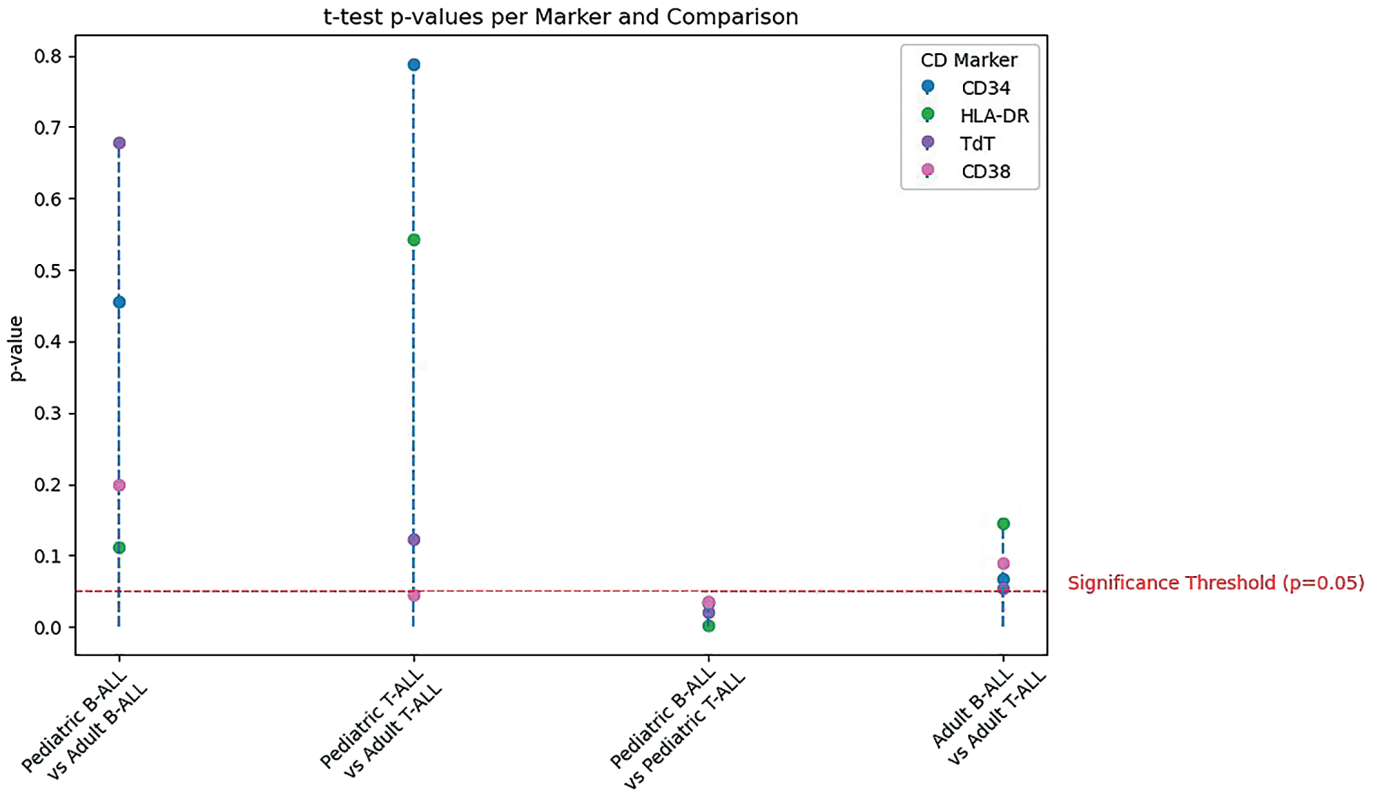

Fig. 2 T-test p-values.

Tab. 6 Mann-Whitney U Tests for CD Marker Expression Between Patient Groups.

CD Marker	p-value (Pediatric B-ALL vs. Adult B-ALL)	p-value (Pediatric T-ALL vs. Adult T-ALL)	p-value (Pediatric B-ALL vs. Pediatric T-ALL)	p-value (Adult B-ALL vs. Adult T-ALL)
CD34	0.025	0.001	0.030	0.019
HLA-DR	0.015	0.067	0.001	0.039
TdT	0.051	0.009	0.019	0.149
CD38	0.022	0.045	0.035	0.080

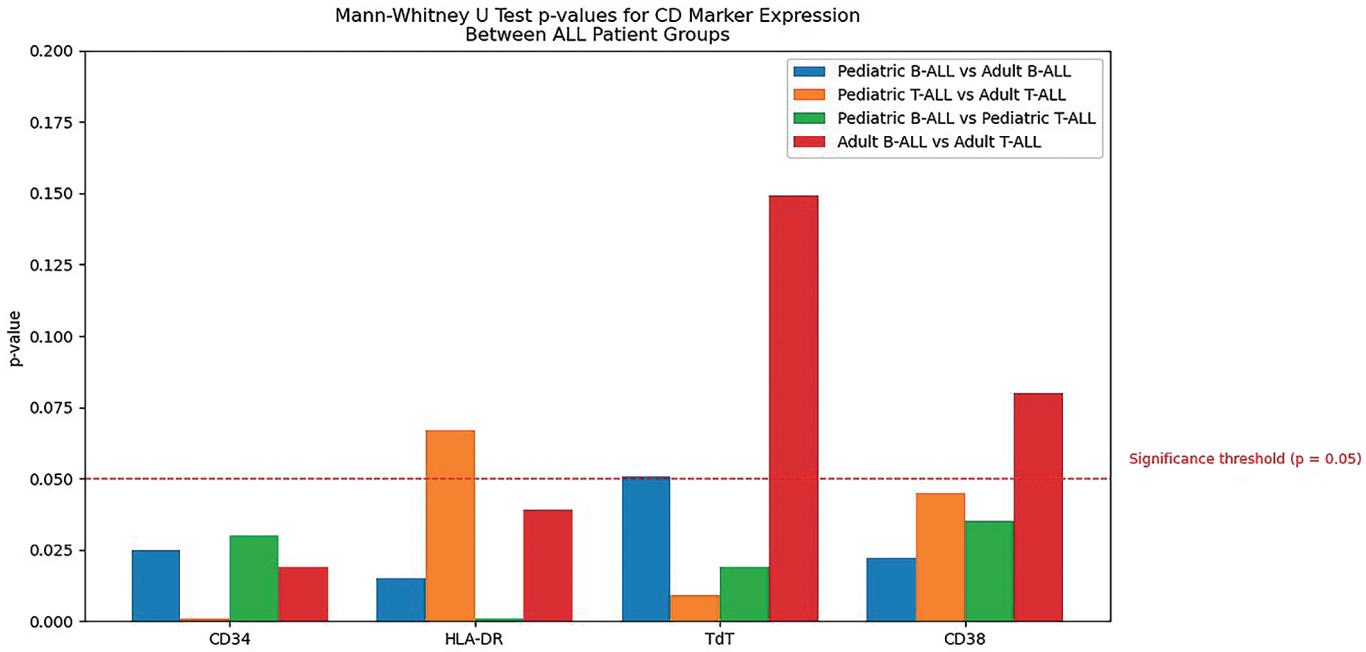

Fig. 3 Mann-Whitney U Test p-values.

Tab. 7 Correlation Analysis Results.

CD Marker	Pediatric B-ALL (51)	Pediatric T-ALL (16)	Adult B-ALL (44)	Adult T-ALL (19)
Pediatric B-ALL (51)	1	0.013295	0.981065	0.134304565
Pediatric T-ALL (16)	0.013295	1	-0.1355	0.892212673
Adult B-ALL (44)	0.981065	-0.1355	1	0.110501866
Adult T-ALL (19)	0.134305	0.892213	0.110502	1

those subtypes concerning CD marker expressions among children. Table 5 shows the correlation results analysis.

In addition, a correlation matrix was constructed to evaluate the relationships between the expression levels of these markers across the different patient groups. A very high positive correlation (r = 0.981) was found between Pediatric B-ALL and Adult B-ALL, suggesting that the immunophenotypic profiles of B-cell ALL are remarkably consistent across age groups. Similarly, a strong positive correlation (r = 0.892) was observed between Pediatric T-ALL and Adult T-ALL, indicating that T-cell ALL maintains similar marker expression patterns in children and adults. In contrast, there was an extremely low correlation (r = 0.013) between Pediatric B-ALL and Pediatric T-ALL, underscoring marked differences in CD marker expression between these two pediatric subtypes. Table 7 presents the detailed results of this correlation analysis.

In addition, another one can note that the low correlation (r = 0.111) between Adult B-ALL and Adult T-All may indicate that the adult subtype has different levels of expression of these antigens as compared with the pediatric one. This analysis highlights the fact that over similar age ranges both subtypes held a more constant pattern for each given subtype (B-cell or T-cell ALL). While these observations show that within-age-group variation remains significant; they emphasize nothing else other than the consistency within rather than between types of leukemia

when considering age varieties. This uniformity validates application concerning classification using certain leukemic blood components like its marker system.

DISCUSSION

The findings from this study help to reveal the core features of ALL in various age groups and different subtypes. One of the most important observed phenomena was related to CD34 and HLA-DR expression patterns. Hence, both pediatric and adult individuals showed high levels of its expression for B-ALL as compared with those for the T-ALL group. This finding is also consistent with previous studies that have shown that it has a poor prognosis since it relates to primitive hematopoietic progenitor cells during early B-cell development as well as supports early B-cell development through homing. Of great importance is the fact that B-ALL patients had higher CD34 expressions similar to a study that highlights the prognostication role played by high CD34 counts in childhood leukemia including infant acute lymphoblastic leukemia. Several possibilities may exist, however, lack of statistically significant differences in CD marker expression between the groups.

The study examined CD38 immaturity marker expression and its patterns alongside other markers. The collected data about CD38 expression strengthened the analysis of ALL immunophenotypic characteristics even though the results were not statistically significant for every group. CD38 serves a dual purpose during cellular activation and differentiation processes and its changing expression patterns might indicate distinctive biological features between subtypes combined with age-related characteristics. The observed data demonstrated that B-ALL expression levels exceeded T-ALL expression profiles of CD38 which matches historical data about its use in B-cell maturation processes. In addition, the correlative evaluation showed that both B-ALL and T-ALL subtypes exhibited similar features among patients from different age groups. The results show pediatric and adult patients with B-ALL share identical immunophenotypic profiles ($r = 0.981$) while pediatric and adult patients with T-ALL show strong similarities ($r = 0.892$). In contrast, the minimal correlation between childhood B-ALL and childhood T-ALL ($r = 0.013$) highlights the clear immunological differences between these subtypes, even within the same age group. As shown in the results of this study, CD markers alone may not fully capture the heterogeneity and complexity of disease among different patient populations. Therefore, it might be necessary to include other molecular and genetic markers for a better understanding of ALL. Moreover, these results imply that individual variations rather than oversimplified group comparisons should inform personalized diagnostic and therapeutic strategies based on marker expressions. The nominally prognostic significance of CD34, HLA-DR, and TdT proteins becomes more valuable for clinical assessments through integration with cytogenetic and molecular assessments across different age groups. The study lacks survival data or outcome measures therefore future research involving long-term study is required to determine how these antigenic expressions influence prognosis. The diagnosis and classification of ALL in high-resource areas depends on molecular genetic analysis together with cytogenetic profiling tests. The areas of Iraq and similar regions conduct their diagnoses primarily using morphology and immunophenotyping because of inadequate infrastructure. The identification of trustable surface markers proves essential for simultaneous diagnosis and future disease classification processes in these settings thus contributing to better standardized medical care.

CONCLUSION

This research examined the quantitative CD marker expressions in pediatric and adult patients with acute lymphoblastic leukemia who had B-ALL and T-ALL cancer types. Flow cytometry data provided information for t-tests along with Mann-Whitney U tests which functioned as parametric and non-parametric tests respectively to detect dissimilarities in the group characteristics. Statistical analyses established significant marker expression disparities between different cell types except for B-ALL and T-ALL comparison where results showed clear CD34, HLA-DR, and TdT variations. Patterns of CD38 showed trends to add understanding to immunophenotypic variations between different patient groups even though statistical significance was not always achieved. Marker expression pattern consistency across pediatric and adult groups within the same subtype received support from descriptive statistics analysis and correlation tests.

The findings demonstrate that ALL exhibits complicated immunophenotypic characteristics which should not lead doctors to rely only on CD marker profiles for diagnostic decisions or predictive outcomes. The accurate diagnosis and individualized understanding of the disease as a future approach requires combining CD markers with molecular and genetic markers throughout ALL classification stages.

REFERENCES

1. Olteanu H. Lymphoblastic Leukemia/Lymphoma. In: Molina TJ, ed. Hematopathology. Encyclopedia of Pathology. Cham: Springer, 2020: 307–15.
2. He Y. Dissecting oncogenic signaling by Bcr/Abl and Notch (Dissertation). Philadelphia, Pennsylvania, United States: University of Pennsylvania, 2002. 141 pp.
3. Gębarowska K, Mroczek A, Kowalczyk JR, Lejman M. MicroRNA as a Prognostic and Diagnostic Marker in T-Cell Acute Lymphoblastic Leukemia. Int J Mol Sci. 2021 May 18; 22(10): 5317.
4. Yaghmaie M, Ahmadvand M, Nejati Safa A, Pashaiefar H. Genetic, Hematologic and Psychological Aspects of Leukemia. In: Mehdipour P, ed. Cancer Genetics and Psychotherapy. Cham: Springer, 2017: 667–755.
5. Mohseni M, Uludag H, Brandwein JM. Advances in biology of acute lymphoblastic leukemia (ALL) and therapeutic implications. Am J Blood Res. 2018 Dec 10; 8(4): 29–56.
6. Ratti S, Lonetti A, Follo MY, et al. B-ALL Complexity: Is Targeted Therapy Still A Valuable Approach for Pediatric Patients? Cancers (Basel). 2020 Nov 24; 12(12): 3498.
7. Porwit A, Béné MC. Multiparameter flow cytometry applications in the diagnosis of mixed phenotype acute leukemia. Cytometry B Clin Cytom. 2019 May; 96(3): 183–94.

8. Emmrich S, Trapp A, Tolibzoda Zakusilo F, et al. Characterization of naked mole-rat hematopoiesis reveals unique stem and progenitor cell patterns and neotenic traits. EMBO J. 2022 Aug 1; 41(15): e109694.
9. Mahapatra S, Mace EM, Minard CG, Forbes LR, et al. High-resolution phenotyping identifies NK cell subsets that distinguish healthy children from adults. PLoS One. 2017 Aug 2; 12(8): e0181134.
10. Gupta M, Monga L, Mehrotra D, Chhabra S, Singhal S, Sen R. Immunophenotypic Aberrancies in Acute Leukemia: A Tertiary Care Centre Experience. Oman Med J. 2021 Jan 31; 36(1): e218.
11. van Grotel M, Meijerink JP, van Wering ER, et al. Prognostic significance of molecular-cytogenetic abnormalities in pediatric T-ALL is not explained by immunophenotypic differences. Leukemia. 2008 Jan; 22(1): 124–31.
12. Karrman K, Johansson B. Pediatric T-cell acute lymphoblastic leukemia. Genes Chromosomes Cancer. 2017 Feb; 56(2): 89–116.

Eyelid Radiotherapy-Treated Basal and Squamous Cell Carcinomas: A Case Series

Ioannis Athanasiadis[1], Aristeidis Konstantinidis[1], Eirini-Kanella Panagiotopoulou[1], Minas Bakirtzis[1,*], Michael Koukourakis[2], Georgios Labiris[1]

ABSTRACT

Introduction: This case report aims to showcase the successful application of electron hypofractionated radiotherapy in the treatment of eyelid basal cell carcinoma (BCC) and squamous cell carcinoma (SCC).

Cases Presentation: Two cases are presented involving a 91-year-old Greek female with nodular BCC and an 88-year-old Greek male with ulcerative SCC. Both cases were treated with electron 10MeV irradiation using an ELEKTA 5-15MV linear accelerator. In the first case, a patient with advanced dementia presented with left-upper-eyelid nodular BCC. Following confirmation through biopsy and imaging, hypofractionated electron-beam radiotherapy was chosen, leading to gradual recession of the lesion and no recurrence at the one-year follow-up. In the second case, an elderly male with comorbidities had right-upper-eyelid ulcerative SCC. After systemic evaluation ruled out metastasis, the patient underwent hypofractionated radiotherapy, resulting in unexpected lesion shrinkage, resolution, and absence of recurrence at the 6-month and one-year follow-ups.

Conclusions: Hypofractionated electron-beam radiotherapy emerges as an effective and well-tolerated alternative for eyelid tumors, particularly in cases where surgical excision is challenging or contraindicated.

KEYWORDS

basal cell carcinoma; squamous cell carcinoma; electron hypofractionated radiotherapy; reverse koebner

AUTHOR AFFILIATIONS

[1] Department of Ophthalmology, University Hospital of Alexandroupolis, Medical School, Democritus University of Thrace, Alexandroupolis, Greece

[2] Department of Radiotherapy and Oncology, University Hospital of Alexandroupolis, Medical School, Democritus University of Thrace, Alexandroupolis, Greece

* Corresponding author: Department of Ophthalmology, University Hospital of Alexandroupolis, Medical School, Democritus University of Thrace, Alexandroupolis, Greece; e-mail: minas961@hotmail.com

Received: 1 February 2025
Accepted: 29 July 2025
Published online: 6 October 2025

Acta Medica (Hradec Králové) 2025; 68(2): 58–62
https://doi.org/10.14712/18059694.2025.20

INTRODUCTION

Basal cell (BCC) and squamous cell carcinomas (SCC) are the two most common malignant neoplasms of the eyelids (1–3). Both BCC and SCC primarily involve the lower lid margin and inner canthus (4, 5). Although BCC is a low metastatic tumor, it is locally destructive and invasive to deeper structures, but rarely intraocularly. If BCC is left untreated, it may result in serious aesthetic and functional implications due to orbital invasion (6). On the other hand, SCC tends to metastasize more often than BCC, with lymph node and distant metastases threatening patients' life (7, 8). It is very important to distinguish them from other eyelid lesions and incisional biopsy is mandatory when there is suspicion of such lesion. If the diagnosis of SCC is confirmed, the patient should be checked extensively for systemic involvement. A series of treatment options have been described for BCC and SCC. The non-surgical options include cryotherapy, radiation, topical 5-fluorouracil, topical imiquimod, and photodynamic therapy. Additionally, systemic therapies have emerged for advanced cases, such as Erivedge (Vismodegibum), a hedgehog pathway inhibitor approved for the treatment of locally advanced or metastatic BCC (9), and Libtayo (Cemiplimabum), a PD-1 inhibitor used in advanced cutaneous SCC (10). These targeted therapies offer alternative treatment options for patients unsuitable for surgery or radiation. However, for both malignancies, surgical excision remains the gold standard therapeutic intervention (11). The treatment of choice depends on the physician's preference and the patient's characteristics.

Radiotherapy (RT) has been established as a viable treatment modality for BCC and SCC, particularly in the periocular area. RT offers several advantages, such as the preservation of anatomical structures and function, making it an appealing option for cases where surgical intervention may pose challenges. Additionally, RT is non-invasive, making it suitable for elderly patients or those with significant comorbidities who may not be ideal candidates for surgery (12, 13).

Despite its advantages, RT for BCC and SCC of the periocular area has its limitations. One of the primary concerns is the potential damage to surrounding healthy tissues, which may lead to adverse effects. Furthermore, the efficacy of RT can be influenced by factors such as tumor size, location, and histological characteristics. Thus, careful consideration and individualized treatment planning are crucial to optimize outcomes and minimize potential complications (14).

The application of hypofractionated radiotherapy has demonstrated effectiveness and excellent tolerability, yielding favorable cosmetic results (15). Additionally, the radiotherapy regimen offers convenience to patients by minimizing the required visits to Radiotherapy centres.

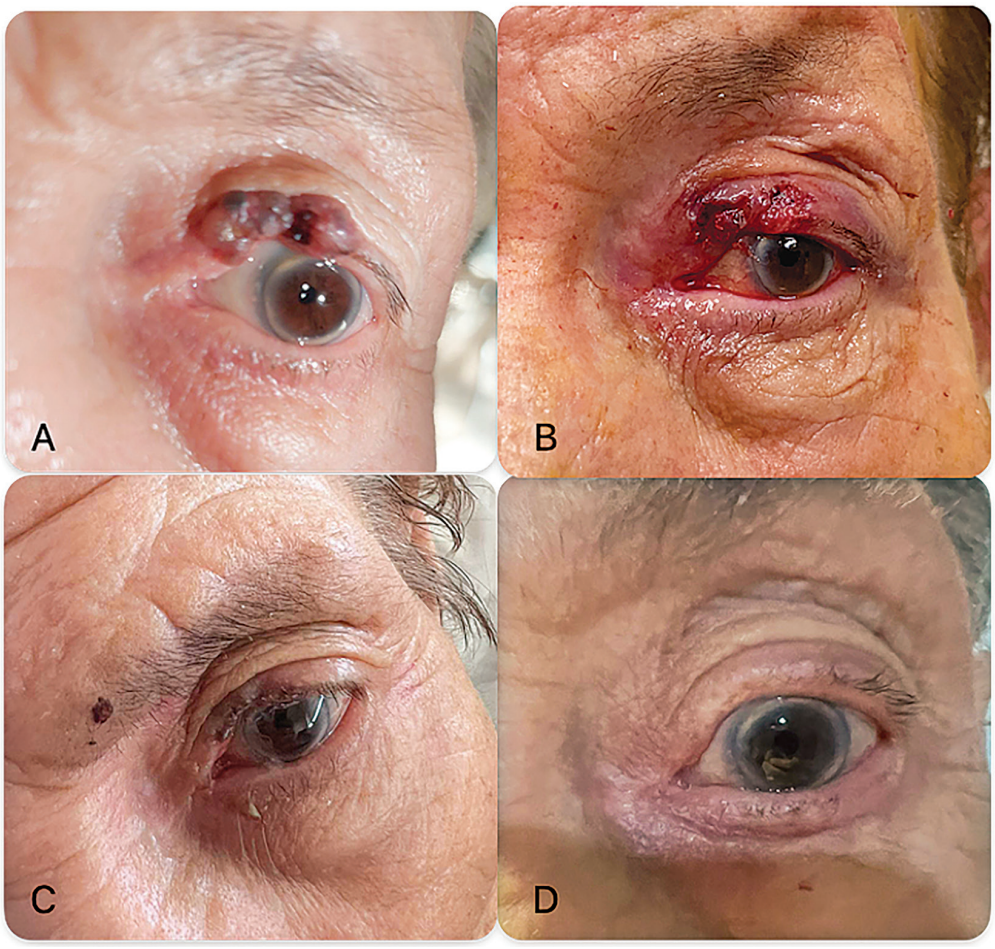

Fig. 1 Basal Cell Carcinoma of the left upper eyelid. A. Preoperative clinical appearance, B. Clinical picture immediately after biopsy, C. 1 week post hypofractionated electron-beam radiotherapy, D. 1-year-follow-up after hypofractionated electron-beam radiotherapy.

Within this context, we present two cases of BCC and SCC, both treated successfully with electron hypofractionated radiotherapy.

CASE PRESENTATION

FIRST CASE

A 91-year-old Greek female was referred to our oculoplastic department in December 2022 for a left-upper-eyelid nodular and ulcerative lesion with well-defined borders, loss of eyelashes, and small telangiectatic vessels on its surface (shown in Fig. 1A). The patient had advanced dementia and no other significant medical history. She was bilaterally pseudophakic with no other ocular pathology. A biopsy was performed and confirmed the presence of nodular BCC (shown in Fig. 1B). Orbit Magnetic resonance imaging (MRI) excluded metastasis to the orbit and neighbouring tissues. Taking into account the age of the patient, the location, and the extent of the lesion, treatment options were discussed with the patient, who opted to undergo radiotherapy. She was then referred for treatment and underwent hypofractionated electron-beam radiotherapy as the best treatment option for her, recommended by the radiotherapist. She was reviewed one week (shown in Fig. 1C) and three months after radiation therapy and showed gradual recession of the lesion. At the one-year follow-up, the patient had no signs of tumor recurrence on clinical examination (shown in Fig. 1D).

SECOND CASE

An 88-year-old Greek male was referred to our oculoplastic department in September 2022 for a right-upper-eyelid large ulcerative lesion (shown in Fig. 2A). Physical examination and slit-lamp biomicroscopy revealed a flat, ulcerative, fleshy, hemorrhagic lesion of about 3 cm in diameter, with irregular borders and scattered necrotic areas. His medical history included cardiac failure, asthma, diabetes mellitus type II, hyperuricemia, and normocytic anemia (with hemoglobin equal to 8.6 g/dL). His ocular history was unremarkable. Histopathological examination of a skin biopsy specimen taken one week later from the lesion showed features consistent with SCC. Therefore, he was first referred to a dermatologist, who suggested head, neck, chest, and abdominal Computed tomography (CT) to stage the tumor and exclude other malignancies. Orbit CT and MRI revealed a 2.7 cm cross-diameter heterogeneously enhanced soft-tissue mass in the right upper eyelid inner canthal area with intact eye globe, free retrobulbar spaces, as well as normal and symmetric imaging of the extraocular muscles and optic nerves bilaterally. A lymph node of 15 mm in diameter was detected in the left supraclavicular region and lymph nodes of marginal diameter were detected in the left axillary area. A non-clearly defined, hypo-enhancing, large liver mass was also detected. The detected lymph nodes and the liver mass were evaluated by radiotherapists and oncologists and were considered random, irrelevant to the skin carcinoma, based on the CT and MRI imaging findings and the radiologists' suggestions. As a result, the full systemic examination turned negative and hypofractionated electron-beam radiotherapy was selected as the most appropriate therapy, taking into consideration the patient's age as well as the extent and the location of the lesion. At the 2-week follow-up after biopsy, the lesion was unexpectedly significantly shrunk (reduction of about 1 cm) (shown in Fig. 2B), which was attributed to possible reverse Koebner phenomenon.

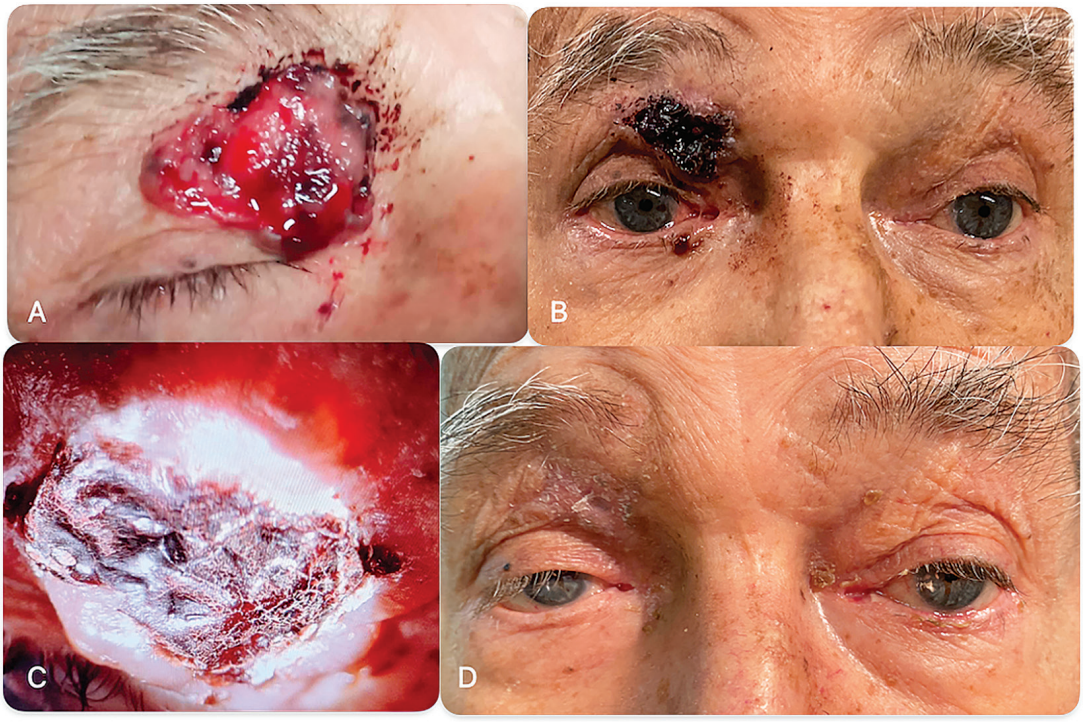

Fig. 2 Squamous Cell Carcinoma of the right upper eyelid. A. First examination in our oculoplastic department, B. two weeks after biopsy, C. one week after radiotherapy, D. four weeks after completing the irradiation cycle.

One week following radiotherapy, the lesion was further reduced in size to approximately 1.5 cm (shown in Fig. 2C). Four weeks after completing the irradiation cycle, an almost complete resolution of the tumor was observed with clinical appearance of scar tissue present (shown in Fig. 2D). A post-radiotherapy biopsy was performed at the 6-month follow-up, which revealed no presence of cancer cells. At the one-year follow-up, the patient had no signs of tumor recurrence on clinical examination.

Both patients were treated with electron 10MeV irradiation, using an ELEKTA 6-15MV linear accelerator. The choice of 10MeV energy was based on the fact that a lower, e.g. 6MeV, beam energy is associated with a 20% reduction of the surface radiation dose, which would demand a 1,5 cm bolus material over the lesion to assure 100% of the dose to the cancer surface. This would allow an adequate dose coverage up to a depth of no more than 1 cm (https://oncologymedicalphysics.com/electron-therapy-physics/). A beam of 10MeV energy on the lesion surface covered by 1–1.5 cm bolus material brings 100% of the radiation dose to the lesion's surface, allowing 90% of the dose to cover a depth of around 1–2 cm to assure inclusion of possible subclinical deep tumor invasion in the high dose area. Thus, a 1–1.5 cm thick bolus material was applied over the lesion before irradiation. A standard electron beam applicator of 6 × 6 cm was used, and lead blocks were applied on the applicator tray to shape the radiation field as demanded. An appropriate angle of the beam direction was considered by rotating the LINAC gantry and/or table to avoid critical structures like the eyeball and lens. The patient was instructed to look at a fixed point to facilitate the maximum possible distancing of the eye lens. According to the underlying tissue/organ, an individualized margin of 0,2–1 cm around the lesion defined the PTV. Narrower margins, for example, were necessary at the areas where the tumor of the eyelid borders the eyeball. The total dose delivered was 36 Gy, with 6 Gy fractions and three fractions per week, within 12 days. There were no adverse events during or after irradiation in either reported case. Mild erythema of no clinical significance was observed, and none of the patients had developed fibrosis, shrinkage, or other complications at the last follow-up.

DISCUSSION

Eyelid skin malignancies, including basal cell carcinoma (BCC) and squamous cell carcinoma (SCC), are among the most frequently encountered tumors in ophthalmic practice (3). They present significant management challenges due to their location and their potential for functional and cosmetic consequences (16). This series presents two cases of eyelid BCC and SCC, treated with electron 10 MeV irradiation, emphasizing the importance of a multidisciplinary approach involving ophthalmologists, dermatologists, pathologists, radiotherapists, and oncologists to ensure optimal patient outcomes, especially when the clinical picture shows advanced signs of the disease.

Both cases presented malignancies in the upper eyelid. It is known that both BCC and SCC mainly involve the lower lid margin and inner canthus. When a skin lesion appears in the upper eyelid and outer canthus, the diagnosis of SCC is more common than the diagnosis of BCC (3). In both cases, the diagnosis was confirmed with a biopsy. Interestingly, a significant reversal of the skin lesion was observed in the second case between the biopsy and the first 20-day follow-up. This is compatible with reverse Koebner response, which is the nonappearance or disappearance of the lesions of particular dermatoses at the site of injury (17). The exact etiopathogenesis of reverse Koebner phenomenon is poorly understood. A few previous reports of reverse Koebner phenomenon are available in the literature for several skin lesions, such as psoriasis, vasculitis, and primary cutaneous follicle center lymphoma following skin biopsy (17–19), however, there is no previous report of reverse Koebner phenomenon in eyelid SCC.

Taking into account the tumors' characteristics, the age and comorbidities of the patient, the patients' preference, as well as the recommendation by the radiotherapist, it was decided to perform electron 10 MeV irradiation in both patients, instead of surgical excision. Kilovoltage or electron beam radiotherapy has been routinely used for the treatment of superficially located tumors, including squamous cell and basal-cell carcinomas (20, 21). Although the first-line therapy of BCC and SCC remains the surgical excision, hypofractionated radiotherapy, as herein applied, has been proved effective and well tolerated, with good cosmetic outcomes (22). Moreover, the radiotherapy schedule is convenient for patients as it reduces the number of visits to the Radiotherapy centers and alleviates the waiting lists in busy departments. The biological dose equivalent to 2Gy (EQD2) for the 6×6Gy schedule is 60Gy, calculated for an α/β-ratio of 4Gy for normal tissue late toxicity (23). Although the EQD2 for a tumor α/β-ratio equal to 10Gy is lower (48Gy), the biological dose is increased due to the acceleration of the overall treatment time by 4 weeks compared to a conventionally fractionated radiotherapy scheme. Assuming a λ-value of 0.5Gy/day for skin cancer, the EQD2 with time correction (EQD2-T) becomes 62Gy.

Skin cancer of the eyelid and periorbital area, whether of squamous or basal-cell histology, is often localized. Although metastasis is infrequent, this mainly involves the preauricular or upper neck lymph nodes. Distant metastasis can evolve in a minority of patients, especially with squamous cell histology, large tumors, and extensive invasion of adjacent anatomical structures (24). Invasion to mediastinal and axillary lymph nodes should be considered exceptional, and the presence of small lymph nodes in these areas should be considered a random, still frequent event in elderly patients, irrelevant to the skin carcinoma. BCC has an extremely low rate of metastasis (0.03%), and the most common sites are the regional lymph nodes and the orbitofacial area (25). On the other hand, SCC tends to metastasize more often than BCC, primarily with preauricular and submandibular lymph node metastases at a rate of 3–6%, and with distant metastases located primarily at the lungs and the parotid gland at a rate of 1% (7, 8, 26).

Radiotherapy, with its ability to precisely target cancerous cells while minimizing damage to surrounding healthy tissue, has proven to be particularly advantageous

in cases where surgery may be challenging due to anatomical considerations or patient preferences. Several studies and clinical experiences have highlighted the successful outcomes of RT in achieving high cure rates for patients with early-stage periocular skin cancer. The effectiveness of RT in achieving local control and minimizing recurrence has established its role as a primary treatment modality for these cases. Additionally, RT has been instrumental in addressing locally advanced tumors, where surgical resection might pose challenges or compromise functional and cosmetic outcomes (20–22).

Although several studies are available in the relevant literature evaluating kilovoltage radiotherapy in eyelid tumors, to our knowledge, this was the first case report presenting cases of BCC and SCC treated with hypofractionated 10MeV electron-beam radiotherapy. Moreover, hypofractionated radiotherapy has been reported as a treatment for skin BCC and SCC (27, 28), however, no previous reports are available for the treatment of eyelid BCC and SCC with hypofractionated radiotherapy. Moreover, although few reports of reverse Koebner phenomenon are available in the literature for several skin lesions, to our knowledge, there is no previous report of reverse Koebner phenomenon in eyelid SCC.

In conclusion, hypofractionated electron-beam radiotherapy seems to be an efficient treatment for patients with eyelid tumors when surgery is absolutely or relatively contraindicated. Moreover, a multidisciplinary approach involving ophthalmologists, dermatologists, pathologists, radiotherapists, and oncologists is suggested to ensure optimal patient outcomes.

STATEMENT OF ETHICS

Ethical approval is not required for this study in accordance with local or national guidelines. Written informed consent was obtained from the patients for publication of this case report and any accompanying images.

FINANCIAL DISCLOSURE

No financial support was received for this case report. None of the authors has any proprietary interests or conflicts of interest related to this submission. It is not simultaneously being considered for publication at any other journal.

REFERENCES

1. Reifler DM, Hornblass A. Squamous cell carcinoma of the eyelid. Surv Ophthalmol. 1986; 30: 349–65.
2. Font RL. Eyelids and lacrimal drainage system. In: Ophthalmic Pathology. An Atlas and Textbook. 3rd ed. Philadelphia, United States: WB Saunders, 1996: 2229–32.
3. Pe'er J. Pathology of eyelid tumors. Indian J Ophthalmol. 2016; 64: 177–90.
4. Person JR. An actinic keratosis is neither malignant nor premalignant: It is an initiated tumor. J Am Acad Dermatol. 2003; 48: 637–8.
5. Brooks BP, Thompson AH, Bishop RJ, et al. Ocular manifestations of xeroderma pigmentosum: Long-term follow-up highlights the role of DNA repair in protection from sun damage. Ophthalmology. 2013; 120: 1324–36.
6. Totir M, Alexandrescu C, Pirvulescu R, Gradinaru S, Costache M. Clinical. Histopathological and Therapeutical Analysis of Inferior Eyelid Basal Cell Carcinomas. J Med Life. 2014; 7: 18–22.
7. Nasser QJ, Roth KG, Warneke CL, Yin VT, El Sawy T, Esmaeli B. Impact of AJCC 'T' designation on risk of regional lymph node metastasis in patients with squamous carcinoma of the eyelid. Br J Ophthalmol. 2014; 98: 498–501.
8. Sun MT, Andrew NH, O'Donnell B, McNab A, Huilgol SC, Selva D. Periocular squamous cell carcinoma: TNM staging and recurrence. Ophthalmology. 2015; 122: 1512–6.
9. Peris K, Fargnoli MC, Kaufmann R, et al. European consensus-based interdisciplinary guideline for diagnosis and treatment of basal cell carcinoma-update 2023. Eur J Cancer. 2023; 192: 113254.
10. Migden MR, Rischin D, Schmults CD, et al. PD-1 Blockade with Cemiplimab in Advanced Cutaneous Squamous-Cell Carcinoma. N Engl J Med. 2018 Jul 26; 379: 341–351.
11. Bonilla R, Solebo AL, Khandwala MA, Jones CA. Imiquimod 5% Cream as an Adjuvant Pre-operative Treatment for Basal Cell Carcinoma of the Periocular Area. Orbit. 2014; 33: 471–3.
12. Sato Y, Takahashi S, Toshiyasu T, Tsuji H, Hanai N, Homma A. Squamous cell carcinoma of the eyelid. Jpn J Clin Oncol. 2024; 54: 4–12.
13. Mudge MC, Green E. Radiotherapy in Equine Practice. Vet Clin North Am Equine Pract. 2024; 40: 397–408.
14. Lazarevic D, Ramelyte E, Dummer R, Imhof L. Radiotherapy in Periocular Cutaneous Malignancies: A Retrospective Study. Dermatology. 2019; 235: 234–9.
15. Tsao MN, Barnes EA, Karam I, Rembielak A. Hypofractionated Radiation Therapy in Keratinocyte Carcinoma. Clin Oncol (R Coll Radiol). 2022; 34: e218–e224.
16. Furdova A, Kapitanova K, Kollarova A, Sekac J. Periocular basal cell carcinoma – clinical perspectives. Oncol Rev. 2020; 14: 420.
17. Yadav S, De D, Kanwar AJ. Reverse koebner phenomenon in leukocytoclastic vasculitis. Indian J Dermatol. 2011; 56: 598–9.
18. Choi B, Tan MG, Gooderham MJ, Beecker J. Reverse koebnerization of primary cutaneous follicle center lymphoma following skin biopsy. JAAD Case Rep. 2021; 16: 149–51.
19. Eyre RW, Krueger GG. Response to injury of skin involved and uninvolved with psoriasis, and its relation to disease activity: Koebner and 'reverse' Koebner reactions. Br J Dermatol. 1982; 106: 153–9.
20. Likhacheva A, Awan M, Barker CA, Bhatnagar A, Bradfield L, Brady MS, et al. Definitive and Postoperative Radiation Therapy for Basal and Squamous Cell Cancers of the Skin: Executive Summary of an American Society for Radiation Oncology Clinical Practice Guideline. Pract Radiat Oncol. 2020; 10: 8–20.
21. Veness MJ, Delishaj D, Barnes EA, Bezugly A, Rembielak A. Current Role of Radiotherapy in Non-melanoma Skin Cancer. Clin Oncol (R Coll Radiol). 2019; 31: 749–58.
22. Tsao MN, Barnes EA, Karam I, Rembielak A. Hypofractionated Radiation Therapy in Keratinocyte Carcinoma. Clin Oncol (R Coll Radiol). 2022; 34: e218–e224.
23. Koukourakis MI, Damilakis J. LQ-based model for biological radiotherapy planning. Med Dosim. 1994; 19: 269–77.
24. Caudill J, Thomas JE, Burkhart CG. The risk of metastases from squamous cell carcinoma of the skin. Int J Dermatol. 2023; 62: 483–6.
25. Ford J, Thakar S, Thuro B, Esmaeli B. Prognostic Value of the Staging System for Eyelid Tumors in the 7th Edition of the American Joint Committee on Cancer Staging Manual. Ophthalmic Plast Reconstr Surg. 2017; 33: 317–24.
26. Xu S, Sagiv O, Rubin ML, et al. Validation Study of the AJCC Cancer Staging Manual, Eighth Edition, Staging System for Eyelid and Periocular Squamous Cell Carcinoma. JAMA Ophthalmol. 2019; 137: 537–42.
27. Zaorsky NG, Lee CT, Zhang E, Keith SW, Galloway TJ. Hypofractionated radiation therapy for basal and squamous cell skin cancer: A meta-analysis. Radiother Oncol. 2017; 125: 13–20.
28. Gunaratne DA, Veness MJ. Efficacy of hypofractionated radiotherapy in patients with non-melanoma skin cancer: Results of a systematic review. J Med Imaging Radiat Oncol. 2018; 62: 401–11.

Beyond the Ordinary: Giant Parotid Oncocytoma and the Complexity of Diagnosis

Burak Kaan İnan[1,*], Altan Argun[1], Saim Pamuk[1], Mehmet Akif Abakay[1], İbrahim Sayın[1], Zahide Mine Yazıcı[1]

ABSTRACT

Parotid oncocytoma is a rare benign salivary gland tumor, often misdiagnosed due to overlapping features with other parotid neoplasms. We present the case of an 87-year-old male with a progressively enlarging right parotid mass, confirmed as oncocytoma through imaging and histopathological analysis. The excised oncocytoma measured approximately 9 cm in its greatest dimension, making it one of the largest parotid oncocytomas reported in the literature to date. This case highlights the diagnostic challenges associated with parotid oncocytomas, the limitations of fine-needle aspiration, and the importance of comprehensive diagnostic tools. Surgical resection was curative, with no recurrence at 12 months.

KEYWORDS

parotid oncocytoma; salivary gland; histopathology; neoplasm

AUTHOR AFFILIATIONS

[1] Department of Otorhinolaryngology & Head and Neck Surgery, Bakırköy Dr. Sadi Konuk Training and Research Hospital, 34147, Istanbul, Turkey

* Corresponding author: Department of Otolaryngology & Head and Neck Surgery, Bakırköy Dr. Sadi Konuk Training and Research Hospital, Zuhuratbaba, Dr. Tevfik Sağlam Street, 11, 34147, Istanbul, Turkey; e-mail: burakkaaninan@gmail.com

Received: 9 January 2025
Accepted: 25 July 2025
Published online: 6 October 2025

Acta Medica (Hradec Králové) 2025; 68(2): 63–66
https://doi.org/10.14712/18059694.2025.21

INTRODUCTION

Oncocytoma is a rare benign salivary gland tumor composed of large epithelial cells known as oncocytes. According to the World Health Organization, oncocytic lesions are histologically classified into three categories: oncocytosis, oncocytoma, and oncocytic carcinoma. Oncocytomas account for only 0.4%–1% of salivary gland tumors, making them among the rarest parotid neoplasms. These tumors, characterized by large oncocytes with abundant eosinophilic cytoplasm, are predominantly found in the parotid gland, often in patients over 60 years old. Although fine-needle aspiration biopsy (FNAB) is commonly used in the initial evaluation of parotid masses, it may be insufficient for an accurate diagnosis – particularly in oncocytic neoplasms – due to cytological overlap with other lesions. While core needle biopsy (CNB) offers improved tissue architecture and higher sensitivity, it can also be inconclusive in oncocytic tumors where the distinction between benign and malignant lesions requires evidence of invasion, which may not be captured in limited samples. Therefore, further investigations such as ultrasound (US), magnetic resonance imaging (MRI), and detailed histopathological evaluation following surgical excision are often necessary. This case report presents an oncocytoma case and compares its clinical, radiographic, and histopathological features with those in the literature. The rarity of parotid oncocytoma and its frequently overlapping features with other benign parotid tumors contribute to frequent misdiagnoses, underscoring the importance of thorough diagnostic evaluation.

CASE REPORT

An 87-year-old male patient presented to our clinic with a swelling in the right parotid gland region, persisting for five years (Fig. 1).

Over five years, the lesion progressively enlarged, ultimately reaching a remarkable size of 9 cm, causing visible facial asymmetry. His medical history included a 35-pack-year smoking history, with no known family history of head or neck cancer. On physical examination, palpation revealed a painless, immobile, firm mass with well-defined borders. The patient did not report any associated symptoms, such as difficulty with speech, chewing, or swallowing, indicating that the mass primarily affected facial appearance.

Before presenting to our clinic, the patient underwent initial evaluations at another hospital, including color Doppler ultrasonography performed at an outside facility, which identified a 58 × 44 mm hypoechoic solid mass with moderate internal vascularization. The fine-needle aspiration biopsy (FNAB) result suggested that the mass was consistent with a Warthin tumor, another benign neoplasm of the parotid gland.

The patient presented to our clinic for the first time approximately one year later, during which time the lesion had progressively increased in size. A repeat color Doppler ultrasonography revealed an 85 × 52 mm hypoechoic solid lesion extending into the right submandibular region and adjacent to the internal jugular vein. Contrast-enhanced MRI demonstrated a well-defined 88 × 65 mm

Fig. 1 Preoperative clinical image of the patient demonstrating a large, asymmetric swelling in the parotid region, consistent with a parotid gland oncocytoma.

Fig. 2 Gross specimen of the excised parotid mass consistent with oncocytoma. The mass exhibits a lobulated, encapsulated appearance with a shiny, reddish-brown surface, and cystic spaces.

mass occupying and expanding the right parotid gland. The mass showed hypointense signals on T1-weighted imaging and mixed signals with linear hyperintense areas on T2-weighted imaging, with intense contrast enhancement.

FNAB findings indicated histopathological features compatible with oncocytic neoplasia. However, the exact diagnosis – whether oncocytosis, oncocytoma, or oncocytic carcinoma – remained uncertain. Based on imaging and histopathological evaluations, surgical resection of the mass was recommended. A superficial parotidectomy was performed, limited to the superficial lobe of the parotid gland, with careful preservation of the facial nerve. The gross surgical specimen measured approximately 9 × 9 cm, confirming the significant interval growth of the lesion over time (Fig. 2)

Microscopic evaluation of the hematoxylin and eosin-stained specimen showed oncocytic cells with abundant eosinophilic granular cytoplasm rich in mitochondria, forming trabecular and acinar structures. No necrosis was observed in the tumor tissue (Fig. 3). Due to the benign nature of the tumor and clear surgical margins, adjuvant chemotherapy or radiotherapy was not administered.

At the 12-month postoperative follow-up, the patient remained recurrence-free, with no signs of facial nerve deficit (Fig. 4).

Written informed consent was obtained from the patient.

DISCUSSION

Oncocytoma is a benign salivary gland tumor characterized by epithelial cells known as oncocytes, which contain abundant eosinophilic cytoplasm and centrally located pyknotic nuclei. As shown in Tandler et al.'s study, these cells contain numerous mitochondria (1). Oncocytes produce low levels of adenosine triphosphate (ATP), leading to increased mitochondrial numbers, a key distinguishing feature of these cells. While the pathophysiology of oncocytoma remains unclear, mitochondrial functional defects are thought to play a role.

Oncocytomas primarily occur in the parotid gland. As noted in the study by Stomeo et al., they can present bilaterally (2), though they are usually unilateral with a slow growth pattern, as seen in our case. Generally non-cystic and encapsulated, these tumors measure less than 5 cm, with rare instances of malignant transformation or local recurrence. Patients are commonly over 60 years of age, with no significant gender preference (3). Özcan et al. and Sepulveda et al. noted that while oncocytomas can rarely arise from the deep lobe, they generally originate from the superficial lobe, as observed in our case (4, 5).

For diagnosis, histopathological confirmation is essential, and imaging techniques such as CT, MRI, and US serve as useful adjuncts. US, as the first-line imaging method for parotid masses, can reveal regular borders and an absence of dystrophic calcifications in oncocytomas, distinguishing them from pleomorphic adenomas, which often have lobulated borders and may exhibit calcifications. Another frequently encountered parotid mass, Warthin tumor, can contain necrotic areas, further aiding differentiation. Similar to studies in the literature on oncocytomas, a hypoechoic mass lesion with internal vascularization was also detected on Doppler US in our case (6).

MRI reports suggest that oncocytomas appear hypointense on T1- and T2-weighted images due to high cellularity and low water content. However, variability in

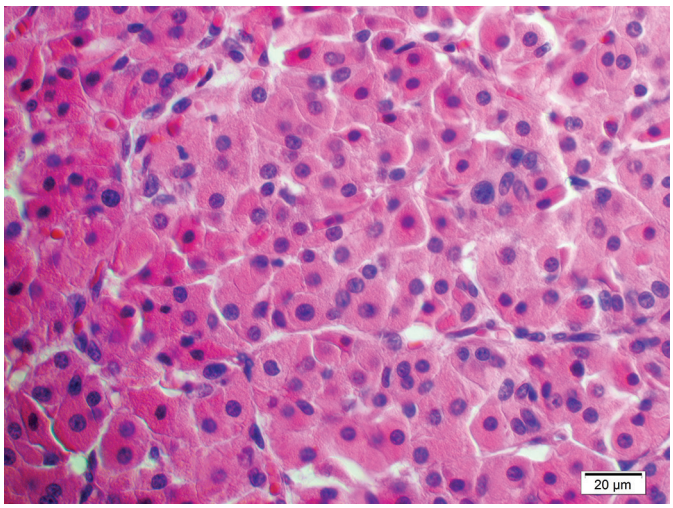

Fig. 3 Histopathological examination revealed oncocytic cells with abundant eosinophilic granular cytoplasm, occasionally forming acinar and trabecular structures. These cells exhibited small, round, centrally located nuclei (H&E, X60).

Fig. 4 Postoperative clinical image of the same patient showing complete resolution of the parotid mass following surgical excision.

MRI appearances exists, as seen in Hamada et al., where oncocytomas appeared hypointense on T1 and iso- to hyperintense on T2 sequences (7). Sepulveda et al. similarly reported isointensity on T1 and hyperintensity on T2 sequences (5). Our case demonstrated hypointense T1 signals and mixed T2 signals with linear hyperintensities, aligning partially with Hamada et al.'s findings but presenting unique radiographic characteristics (7).

FNAB is commonly employed as an initial diagnostic tool in many clinics due to its minimally invasive nature. However, FNAB has significant limitations in accurately diagnosing oncocytomas, particularly due to their overlapping cytological features with other oncocytic lesions. Chakrabarti et al. highlighted the diagnostic challenges FNAB presents in distinguishing oncocytic lesions (8). Diouf et al. reported a case initially misdiagnosed as pleomorphic adenoma, while Miladinovic et al. documented a misinterpretation of parotid oncocytoma as metastatic squamous cell carcinoma based on FNAB findings (9, 10). Furthermore, Capone et al. demonstrated that the sensitivity of FNAB in diagnosing parotid masses is only 29%, underscoring its limitations (3). In our case, the initial FNAB result suggested a Warthin tumor rather than an oncocytoma, consistent with reports in the literature where oncocytomas are often misdiagnosed as other benign parotid tumors. (9) Although both are benign neoplasms, Warthin tumors can be distinguished from oncocytomas by their histological structure, which includes cystic spaces filled with lymphoid stroma. These findings emphasize the need for advanced diagnostic methods. Techniques such as core needle biopsy or intraoperative frozen section analysis could significantly improve diagnostic accuracy by providing more extensive tissue samples and allowing real-time histopathological evaluation.

Though facial nerve involvement typically suggests malignancy in parotid masses, benign parotid tumors like oncocytoma can, on rare occasions, cause facial paralysis, as reported by Hamada et al. (7). Consistent with the benign nature of oncocytomas, our patient exhibited no facial paralysis. The primary treatment for parotid oncocytoma is surgical resection, either radical or superficial parotidectomy, as performed in our case with preservation of the facial nerve (5). Follow-up showed no evidence of recurrence, reinforcing surgical excision as an effective approach.

CONCLUSION

Our case represents the largest reported parotid oncocytoma to date, underscoring the importance of considering parotid oncocytoma in the differential diagnosis of parotid masses. This case not only highlights the diagnostic challenges associated with parotid oncocytomas but also emphasizes the need for advanced imaging and histopathological techniques to accurately identify these rare tumors. Histopathological confirmation, in conjunction with imaging, is crucial for accurate diagnosis. Surgical intervention remains the primary treatment, and close postoperative follow-up is essential to monitor for recurrence.

MAIN POINTS

- Oncocytoma is a rare benign tumor of the salivary glands, most commonly occurring in the parotid gland and often affecting patients over 60 years old.
- Fine-needle aspiration biopsy has significant limitations in accurately diagnosing oncocytoma, often leading to misdiagnosis as other benign tumors like Warthin tumor or pleomorphic adenoma.
- Imaging modalities such as MRI and ultrasound are essential for evaluating parotid masses, but definitive diagnosis requires histopathological examination.
- Surgical resection, typically superficial parotidectomy with facial nerve preservation, is the primary treatment for parotid oncocytomas.
- Close postoperative follow-up is crucial, as although oncocytomas are benign, recurrence is possible in rare cases.

REFERENCES

1. Tandler, B. Fine structure of oncocytes in human salivary glands. Virchows Arch Path Anat. 1966; 341: 317–26.
2. Stomeo F, Meloni F, Bozzo C, et al. Bilateral oncocytoma of the parotid gland. Acta Otolaryngol. 2006; 126(3): 324–6.
3. Capone RB, Ha PK, Westra WH, et al. Oncocytic neoplasms of the parotid gland: a 16-year institutional review. Otolaryngol Head Neck Surg. 2002; 126(6): 657–62.
4. Özcan C, Talas D, Görür K, et al. Incidental deep lobe parotid gland oncocytic neoplasms in an operated larynx cancer patient. Oral Oncol Extra. 2006; 42: 235–40.
5. Sepúlveda I, Platín E, Spencer ML, et al. Oncocytoma of the parotid gland: a case report and review of the literature. Case Rep Oncol. 2014; 7(1): 109–16.
6. Corvino A, Caruso M, Varelli C, et al. Diagnostic imaging of parotid gland oncocytoma: a pictorial review with emphasis on ultrasound assessment. J Ultrasound. 2021; 24(3): 241–7.
7. Hamada S, Fujiwara K, Hatakeyama H, et al. Oncocytoma of the Parotid Gland with Facial Nerve Paralysis. Case Rep Otolaryngol. 2018; 2018: 7687951.
8. Chakrabarti I, Basu A, Ghosh N. Oncocytic lesion of parotid gland: A dilemma for cytopathologists. J Cytol. 2012; 29(1): 80–2.
9. Diouf MS, Ndiaye C, Diongue O, et al. Oncocytoma of the parotid gland: a case report. Rev Laryngol Otol Rhinol (Bord). 2012; 133(2): 109–12.
10. Miladinovic D, Trautman J, Yabe T. A Cautionary Tale: A Case Report Describing a Benign Parotid Oncocytoma Diagnosed as Metastatic Squamous Cell Carcinoma on Fine Needle Aspirate. Cureus. 2023; 15(12): e50853.

EUS Guided FNA Cell Block Cytology and Intraoperative Squash Cytology in the Diagnostic Approach of Unfamiliar Malignant Neoplastic Disorders

Alexandra Kalogeraki[1], Dimitrios Tamiolakis[2,*], Eleni Moustou[1], Evangelos Kalaitzakis[2]

ABSTRACT
Endoscopic ultrasound guided fine needle aspiration cytology (EUS-FNAC) with the employment of cell block preparations and intraoperative squash smear cytology upgrade the interpretation accuracy and typing of common malignant lesions. Yet, their capacity in the diagnostic workup of less familiar neoplastic entities is not clearly determined and this analysis was designed towards this direction. We describe four cases of patients with uncommon malignancies and evaluate EUS-FNA cell block cytology and intraoperative squash smear cytology as a necessary (important) step in rendering the diagnosis. All cases enhance the diagnostic role of cytology in a wide variety of neoplastic disorders including lymphoproliferative conditions and rare carcinomas.

KEYWORDS
EUS-FNAC; DLBCL; osteoclast like giant cell undifferentiated pancreatic tumor; squash cytology; ependymoma; glioma

AUTHOR AFFILIATIONS
[1] Departments of Pathology-Cytopathology, Medical School, University of Crete, University Hospital, Heraklion, Crete, Greece
[2] Gastroenterology, Medical School, University of Crete, University Hospital, Heraklion, Crete, Greece
* Corresponding author: Gastroenterology, Medical School, University of Crete, University Hospital, Heraklion, Crete, Greece; e-mail: dtamiolakis@yahoo.com

Received: 31 March 2025
Accepted: 12 August 2025
Published online: 6 October 2025

Acta Medica (Hradec Králové) 2025; 68(2): 67–72
https://doi.org/10.14712/18059694.2025.22

INTRODUCTION

A number of tumor and tumorlike conditions are considered to present a particular diagnostic hazard in anatomic pathology. EUS-FNA cell block cytology and intraoperative squash smear technique provide multiple and extensive sampling and/or sampling of not neighboring areas of an unfamiliar lesion to determine its heterogeneity.

Endoscopic ultrasound fine needle aspiration (EUS-FNA) permits the examination of the retroperitoneum for lymph nodes as well as pancreatic sampling for neoplastic lesions and the acquisition of cytologic specimens for interpretation (1, 2). Cell blocks contain residual material fragments unsuitable for processing by cytologic techniques but suitable for processing by histologic methods.

Even though architectural structure is missed, cytomorphological features combined with immunocytochemistry and molecular analysis on cell block preparations can render an accurate diagnosis of neoplastic conditions. Specimen sufficiency, tumor morphological appearances, endoscopist's skillfulness and cytopathologist's experience enhance diagnostic capacity.

Intraoperative diagnosis is imperative in neurosurgery and squash cytology provides the neurosurgeon with rapid and accurate results (3). Squash smear cytology is applied upon minimal tissue pieces, permits efficient evaluation of the cellular architecture, detailed morphological features of the cells, provides adequate sampling for immunocytochemical analysis and lacks the ice artifacts of frozen sections. Limitations include failure to manage thickness, crushing artifacts and inappropriate smearing.

EBV related DLBCL arising in the retroperitoneum is infrequent. Traditionally it is diagnosed by histomorphology, immunohistology and flow cytometry of tissue specimens obtained at laparoscopy or open surgery.

Osteoclast like giant cell undifferentiated pancreatic carcinoma is rare. It is also diagnosed by laparoscopically obtained biopsies or at open surgery.

EUS guided FNA cytology combined with immunocytochemical study on cell block preparations provide an accurate diagnosis of retroperitoneal and pancreatic lesions.

Ependymomas in childhood follow astrocytomas and medulloblastomas in frequency of CNS tumors. They originate most commonly in the posterior fossa of the brain and show significant morphological heterogeneity. Astrocytomas compose a large and heterogenous category of CNS tumors. They demonstrate a wide variety in clinical incidence, morphologic features and biologic course.

Both ependymomas and astrocytomas rarely exfoliate neoplastic cells in cerebrospinal fluid specimens. They can be accurately diagnosed in intraoperatively, on demand by the neurosurgeon for rapid diagnosis, prepared squash smears.

Our objective is to highlight the performance of EUS guided FNA cell block cytology in interpretating retroperitoneal and pancreatic lesions as well as to stress the yield of intraoperative squash smear cytology and establish the specific cytological diagnostic criteria in CNS neoplasms.

CASE SERIES

CASE 1. RETROPERITONEAL EBV POSITIVE DLBCL

A 73-year-old female presented with recent-onset artypical abdominal pain and change in bowel habits (alterating conticipation and diarrhea). Her physical examination was normal. Her past medical history included Billroth II surgery without antrum resection, due to peptic ulcer disease 30 years before presentation. She also suffered from rheumatoid arthritis and dyslipidaemia. She received hydrochloroquine, gabapentin, and a statin on a daily basis. An abdominal CT scan revealed multiple retroperitoneal lymph nodes and suspected thickened gastric wall at the level of the antrum. Upper GI tract endoscopy with gastric biopsies as well as ileonoscopy were uneventful. EUS was performed with a curved linear array endoscope (GF-UCT 140 Olympus Medical Europe, Hamburg Germany) under conscious sedation with midazolam and pethidine, in order to examine the gastric wall and obtain cytopathology material from the retroperitoneal lymph nodes.

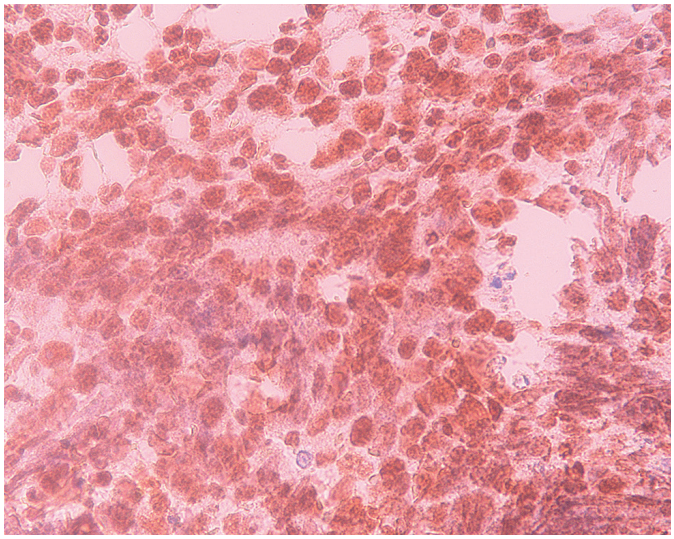

Fig. 1 EBV-DLBCL Cell block preparation. LMP-1 X 400.

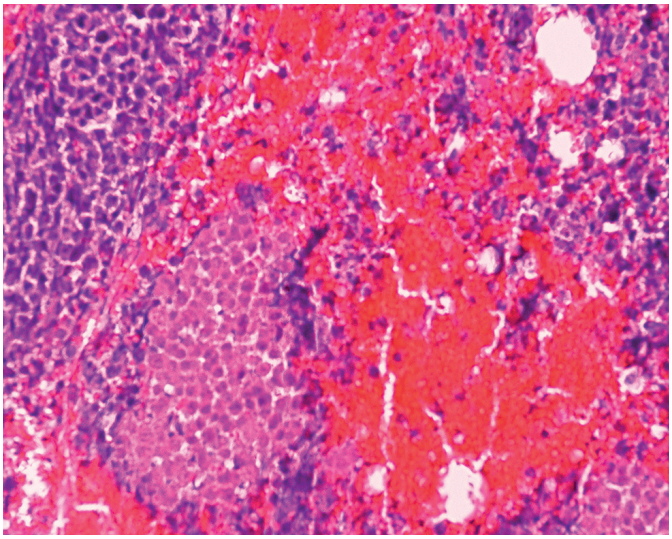

Fig. 2 EBV-DLBCL Cell block preparation. H&E X 200.

On EUS the gastric wall was found of normal thickness with preserved architecture Several enlarged lymph nodes with suspicious EUS features were seen in the retroperitoneum. An EUS guided FNA of a suspicious node was performed through the gastric wall using a 22-gauge needle (Expect Slimline, Boston Scientific, MA) and three passes were made. Suction was applied (10ml vacuum) in the way, and the sample was expelled in normal saline. Soon afterwards it was transferred to the cytopathology lab. The aspirated material was set on smears and air dried, and alcohol fixed slides were prepared. and stained by the Giemsa and Papanicolaou methods respectively A cell block was made from the residual tissue fragments, using the fibrin clot method and it was formalin fixed, and paraffin embedded. Subsequently 5μm thick sections were obtained and stained with hematoxylin and eosin. Additional sections from the cell block were prepared for immunocytochemical analysis.

EUS-FNA conventional and cell block smears showed numerous isolated or clustered large atypical cells with high nuclear cytoplasmic ratio, unevenly distributed chromatin (coarse, granular) and visible nucleoli. The differential diagnosis included metastatic carcinoma, metastatic melanoma, DLBCL, Hodgkin's lymphoma, and anaplastic large cell (ALK-1 positive or negative) lymphoma. Immunocytochemical analysis with the employment of cytokeratin AE1/AE3, HMB45, LCA, CD20, CD3, PAX5, CD30, BCL2, BCL6, MUM-1, CD10, ALK-1, LMP-1 and MIB-1, showed a strong positivity for LCA, CD20, PAX5, BCL2, BCL6, MUM-1, CD10 and LMP-1 and a negative reaction with cytokeratin AE1/AE3, HMB45, CD3, ALK-1,and CD30 of the neoplastic cells. MIB-1 index was 90% positive. A cytological diagnosis of EBV positive DLBCL was established.

CASE 2. OSTEOCLAST LIKE GIANT CELL UNDIFFERENTIATED PANCREATIC TUMOR

Undifferentiated pancreatic carcinoma is an uncommon and aggressive variety of ductal adenocarcinoma. It is categorized in 2 types according to WHO 2019 classification: Undifferentiated carcinoma (with 3 variants: anaplastic, sarcomatoid, and carcinosarcoma) and Undifferentiated carcinoma with osteoclast-like giant cells (OGCT). EUS provides high resolution images and FNA sampling of the pancreatic lesions, which gains a high level of diagnostic accuracy nowadays. OGCTs are large and circumscribed and are defined by non-neoplastic phagocytic cells, large pleomorphic mononuclear cells and small spindled or histiocytoid tumor cells that are usually overlooked in the background. Giant cells are CD68 and Vimentin positive, Cytokeratin and p53 negative, and represent benign histiocytic cells. Pleomorphic mononuclear cells and small spindled cells are strongly positive by Vimentin, variably positive by Cytokeratin and p53, negative by INI-1 (which is strongly positive in Undifferentiated carcinoma lacking giant cells), negative by S-100, and exhibit a high ki-67 proliferation index. The progression from dysplastic epithelium to invasive pancreatic carcinoma is well described because of genetics. KRAS, CDKN2, TP53, and SMAD4 genes are involved in the classical ductal adenocarcinoma while KRAS genetic alterations are frequent in OGCT. Pancreatic mucinous tumor (PaMCT), intraductal papillary mucinous tumor (IPMT), pancreatic cystic neuroendocrine tumor (PaNET), solid pseudopapillary neoplasm (SPN), undifferentiated pancreatic carcinoma not otherwise specified (UOC-NOS), gastrointestinal stromal tumor (GIST), undifferentiated rhabdoid pancreatic tumor (URhT), metastatic melanoma, metastatic sarcoma and chronic pancreatitis with granulation tissue formation are considered in the differentials. PaMCT, IPMT may coexist with OGCC. Cystic degeneration may be present in OGCC, and this can cause a radiologic misinterpretation or may limit sampling from the solid tumor component, so it is critical to ensure that mucinous cystic lesions are extensively sampled. OGCCs may protrude as polyps into the pancreatic or bile duct, duodenum or ampulla and may be also misdiagnosed radiologically. UOC-NOS, URhT do not contain giant cells,.PaNET shows plasmacytoid cells with salt and pepper chromatin, SPN shows open chromatin and nuclear grooves. GIST is c-kit positive. Melanoma stains positive for Melan A, S-100, and HMB45.Sarcoma does not express epithelial markers. Pancreatitis with

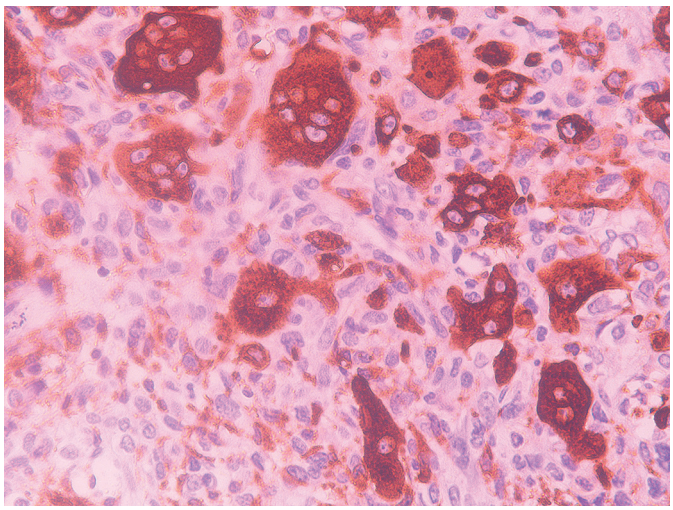

Fig. 3 Osteoclast like giant cell undifferentiated pancreatic tumor. CD68 immunostain X 400.

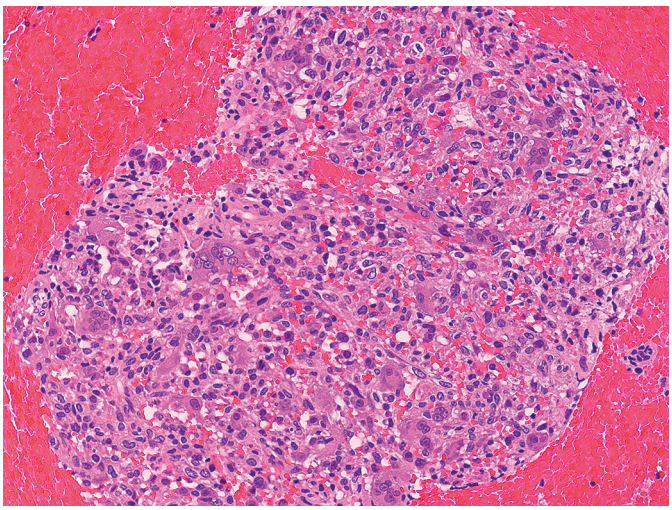

Fig. 4 Osteoclast like giant cell undifferentiated pancreatic tumor. Tissue section X 200.

granulation tissue formation does not express neither epithelial nor vascular (CD31), nor lymphoid markers (ALK), nor S-100, nor c-kit, for neoplastic cells.

An 80 aged female was admitted due to jaundice and epigastralgia. Her past medical. history included arterial hypertension, cardiac arrhythmia, asthma, and chronic frenal failure. CT scan showed a 12mm tumorlike lesion in the head of pancreas which obstructed the common bile duct causing dilatation. EUS revealed a 3,5 hypoechoic heterogeneous poorly defined mass in the pancreatic head. EUS-FNA conventional and cell block slides demonstrated atypical pleomorphic mononuclear cells admixed with multinucleated osteoclast like giant cells with multiple nuclei and ill defined nucleoli. The mononuclear cells were positive by cytokeratin AE1/ AE3, EMA, and CEA but negative by S-100 and c-kit. The multinucleated cells were CD68 positive. A cytological diagnosis of osteoclast like giant cell pancreatic tumor was rendered.

CASE 3. CEREBROSPINAL FLUID AND INTRAOPERATIVE SQUASH CYTOLOGY OF CHILDHOOD EPENDYMOMA

A 19 months old female presented at The University hospital of Heraklion, Crete, Greece in a hemicoma and was intubated. MRI disclosed a tumor in the posterior fossa. The haematological and biochemical work-up was within normal counts. A diagnostic paracentensis was determined and CSF sample was obtained for cytological evaluation. Cytological smears were prepared after cytocentrifuging for 5 minutes. Microscopic interpretation of slides demonstrated isolated neoplastic cells with medium sized oval nuclei and basophilic cytoplasm. Nucleoli or mitotic figures were absent. Dysgerminoma, medulloblastoma, glioma, ependymoma and lymphoma were encountered in the differentials. Neoplastic cells were positive by GFAP and S-100 immunostain but negative by AFP, β-HCG, synaptophysin and LCA. The diagnosis was of a glial tumor favoring ependymoma, based on the age and the anatomical site of the mass. Intraoperative squash preparations were obtained as follows: 1–2 mm^3 of fresh tissue from the suspicious area after gross examination was crushed between two slides to fix smears (4, 5). In squash preparations atypical cells were abundant, organized in papillary formations or rosettes or pseudorosettes with oval medium or large sized nuclei and scanty cytoplasm stained basophilic. GFAP and S-100 positive enhancing the CSF diagnosis of ependymoma. Histological slides showed numerous neuroepithelial neoplastic cells in a rosette-pseudorosette architecture with oval basophilic nuclei and mild atypia. Focally high cellularity, severe nuclear atypia and mitoses were found. Atypical cells were reactive with GFAP, S-100, CD36 and negative for synaptophysin, CD99, CK AE1/AE3. The Ki-1 proliferation index was 10%. Histological diagnosis was of ependymoma WHO grade II and focally grade III (anaplastic) (WHO 2016 earliest classification). The patient was administered with chemotherapy (first course) VEC (vincristine, etoposide and cyclophosphamide).

CASE 4. INTRAOPERATIVE SQUASH CYTOLOGY OF DIFFUSE GLIOMA NOT OTHERWISE SPECIFIED OF THE CEREBELLUM

A 48 aged female was hospitalized at the University hospital of Heraklion, Crete, Greece suffering from headache and unsteadiness. She was soon afterwards diagnosed of a tumor arising in the cerebellum by MRI. Past personal and family medical history was free. Haematological and biochemical values were normal. Intraoperative squash preparations cytological examination demonstrated the presence of isolated elongated epithelial-like neoplastic cells with ovoid nuclei and scanty cytoplasm. Mitoses and necrosis were not observed. Glioma, ependymoma, medulloblastoma and teratoid/rhabdoid tumor were included in the differentials. Immunocytochemical analysis showed a positive cytoplasmic expression of GFAP and a positive expression of S-100 by the tumor cells. Gross total resection of the tumor was performed and histological examination revealed medium sized cells with spindle shaped or oval nuclei, rare mitotic figures and neoangiogenesis. Atypical cells were GFAP podsitive (cytoplasmic positivity), S-100, and vimentin positive,but negative for synaptophysin, NF, EMA,CD34 and p53 antibodies. MIB-1 proliferation index was 5% positive. IDH status and 1p/1q status

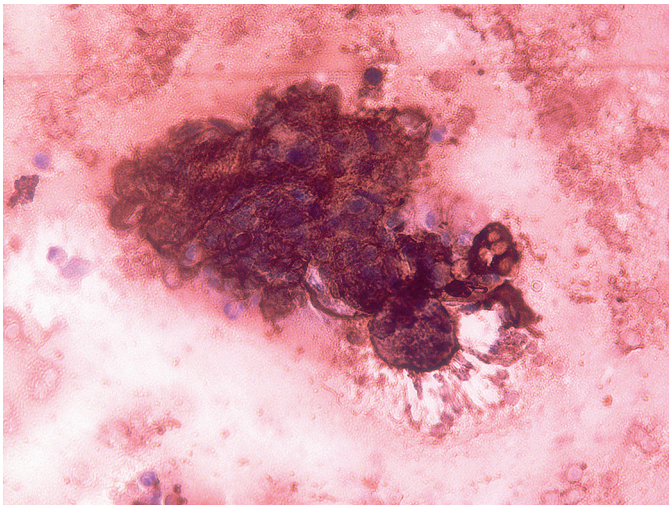

Fig. 5 Ependymoma. Squash smear. GFAP immunostain X 400.

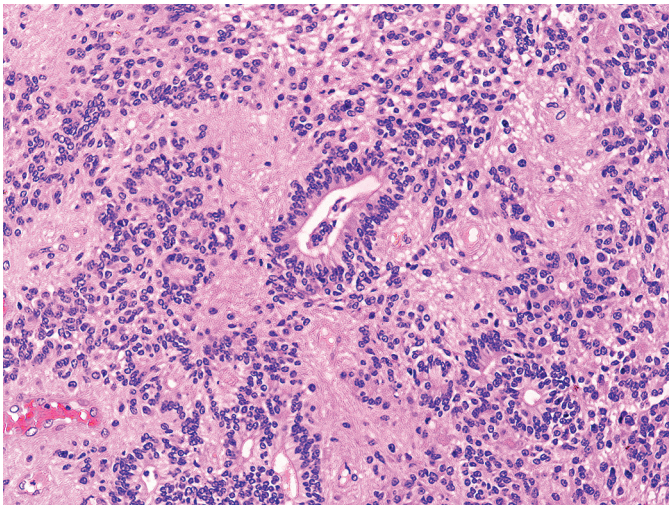

Fig. 6 Ependymoma. Tissue section H$E X 200.

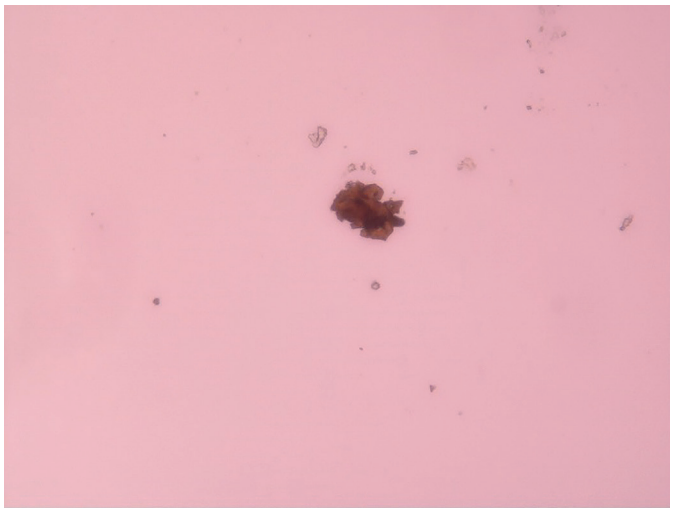

Fig. 7 Low grade glioma of the Cerebellum. Cytological squash smear. GFAP immunostain X 400.

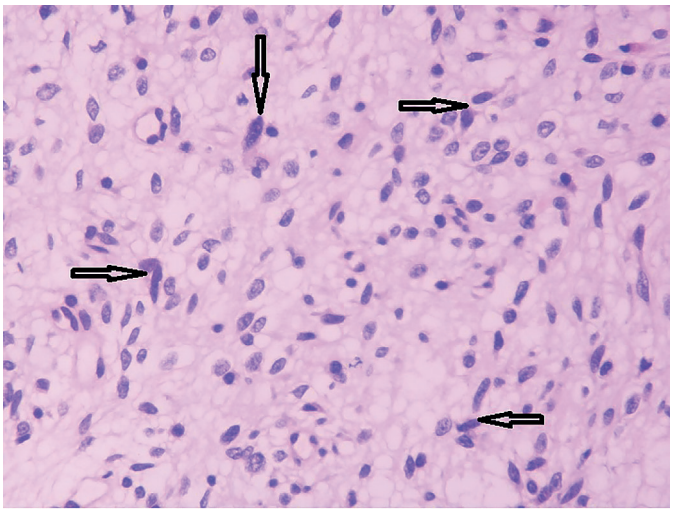

Fig. 8 Low grade glioma of the Cerebellum. Tissue section H&E X 400.

were determined by molecular study and the patient received RT (54 Gy/39 fractions (fr)) followed by 6 courses of PCV (procarbazine, CCNU = lomustine, vincristine) chemotherapy. She is disease free 5 months after surgery.

DISCUSSION

EUS-FNA is a minimally invasive method winning more and more popularity in the nonsurgical appraisal of retroperitoneal lymphoproliferative lesions because of increased accuracy and low morbidity and mortality compared to surgery (6–13).

Echo-findings are important for the evaluation of lymph nodes during EUS, but criteria for malignancy are yet to be established (10, 13). Catalano et al (14) have suggested a number of features such as hypoechoic, sharp borders, rounded contour and size over 10 mm, suggesting malignancy, however this is not always the case as reported by others. In a study by Wang et al (6) enlarged nodes due to lymphoma, were featured by lesion fusion and homogeneous echogenecity. The acquisition and preparation of EUS-FNA samples are critical in the procedure performance because even the most excellent performed aspiration may be wasted if the handling of the specimen is incorrect (15). Three aspirations (passes) of the needle are adequate for the diagnostic yield, a 22 gauge needle is preferred for cytological sampling, the use of forceps enhances the diagnostic yield in lymphoproliferative disorders, the use of suction does not affect the diagnostic yield, neither the use of general anesthesia or sedation nor the number of needle movements from the proximal to distal side of the node (15). The cell block method employs the process of small tissue fragments from aspirated material to form a paraffin block. Cell block slides represent the best material for immunocytochemical and molecular analysis.

There are several drawbacks in the technique for the interpretation of lymphoma: The diagnosis of Hodgkin's lymphoma amends integration of cytomorphology, immunophenotypically, and clinical characteristics so it continues to favor open biopsies for interpretation and classification. T cell lymphoma when occurring (usually rare) also needs open biopsy for the diagnosis. There is need for more than 3 passes from several angles of the lymph node to obtain adequate sampling. Additionally, avoiding necrotic tissue and blood contamination is an important issue (11–13).

Obtaining tissue specimens from pancreatic lesions is considered difficult with CT/ultrasound guided FNA and diagnostic laparoscopy (2). The proximity (accessibility) of the echo-endoscope within the gastrointestinal lumen to the pancreas allows for accurate imaging of the pancreas from the duodenum and the stomach. Sensitivity and specificity of the method is higher (2). EUS-FNA is also effective in patients with inconclusive ERCP brushing cytology (2). The presence of an onsite cytopathologist for rapid onsite evaluation (ROSE) is tremendously improving the diagnostic yield of this technique (2, 15–19). Rapid onsite evaluation (ROSE) with cytology preparations is important in minimally invasive procedures. ROSE activity upgrades patient care by reducing the number of repeat procedures. This reduction saves from potential side effects, such as infection, hemorrhage, and pneumothorax in lung biopsies. ROSE with cytology preparations is also useful in core biopsies (CB) as it minimizes the loss of material that could have been wasted during frozen section analysis. Yet, it decreases the patient anxiety when a procedure does not yield the adequate material or the hazard on the patient by avoiding unnecessary admissions to the clinic. Also, complex oncologic specimens often require fast feedback for clinical management and ancillary studies. ROSE with cytological preparations is performed by cytologists that have to go to the site where the procedure is being performed. The personnel stay on-site until the diagnostic material is obtained or the specimen is considered adequate. The time spent performing ROSE can extend to hours if the lesion is in a location not easy to access and these procedures are managing depended. The standby of the performer cannot be repaid, and it may influence the proceedings of cytology services (25). In our department we do not employ ROSE due to the lack of personnel.

Moreover, ancillary studies and other testing including flow cytometry or culture can be employed (2, 11–13).

Intraoperative diagnosis of brain tumors routinely employs frozen sections. However, they produce artifacts including ice crystals and water logging in the tissue resulting in a smudgy, foggy and shattered tissue appearance (3, 19). Additionally frozen brain tissue displays artifacts in paraffin sections (3, 5, 19). Cytology may sample much wider areas, different areas, and different depths are examined (3, 5, 19).

Definition of brain tumors requires clinical information (patient's age and gender, location of the lesion), medical history, and CT scan or MRI findings. A good cytological squash preparation produces high cellularity, crisp nuclear and cytoplasmic details and occassionaly tissue architectural pattern. In our case of ependymoma, rosette or pseudorosette formation was a critical tip. Limitations include difficulties in preparing smears when lots of intracellular collagen or fibers cannot be spread into slides and this is the case with meningiomas, schwannomas and low grade gliomas (astrocytomas) (5, 19–22). Immunocytochemical and molecular analysis is easy to perform and enhances the diagnostic yield (5, 19–22). Again, the presence of an onsite cytopathologist for ROSE is imperative for improving accuracy. Intraoperative smears of neurosurgical specimens permit rapid and accurate diagnosis (5, 19–22). Cytological assessment should always be followed by histological confirmation (23). Cytological intraoperative report must provide a preliminary accurate diagnosis and assure the neurosurgeon that representative pathological tissue has been obtained for histological definite diagnosis (23, 24).

Our cases facilitate the diagnostic capabilities of EUS-FNA cell block cytology and intraoperative squash cytology over a wide spectrum of neoplasms including unfamiliar lymphoproliferative disorders and carcinomas.

In conclusion the employment of EUS-FNA cell block cytology reinforces an accurate approach of retroperitoneal lyhmphoproliferations and pancreatic lesions utilizing immunocytoclemical and molecular analysis and intraoperative squash cytology can be reliable as the combined skills and flexibilities the management group including the neurosurgeon, the radiologist, and the cytopathologist in the interpretation of brain tumors.

REFERENCES

1. Tanisaka Y, Ryozawa S, Kobayashi M, et al. Usefulness of endoscopic ultrasound guided fine needle aspiration foe lymphadenopathy. Oncol Lett. 2018; 15: 4759–66.
2. Mehmood S, Jahan A, Loya A, Yusuf MA. Onsite Cytopathology Evaluation abd Ancillary studies beneficial in EUS-FNA of pancreatic, mediastinal, intra-abdominal and submucosal lesions. Diagn Cytopathol. 2014; 43(4): 278–86.
3. Panth R. A systematic approach to cytological evaluation of central nervous system tumors. J Pathol Nepal. 2011; 1: 136–41.
4. Adams JH, Graham DI, Doyle D. Brain Biopsy: The Smear Technique for Neurosurgical Biopsies. London: Chapman and Hall, 1981: 11–4.
5. Sarkar S, Sengupta M, Datta Ch, Chatterjee U, Ghost SN. Evaluation of intraoperative cytological smears for diagnosis of brain tumors with special reference to immunohistochemistry. Indian J Med Paediatr Oncol. 2017; 38(3): 296–301.
6. Wang J, Chen Q, Wu X, Wang Y, Hou W, Cheng B. Role of endoscopic ultrasound guided fine needle aspiration in evaluating mediastinal and intra-abdominal lymphadenopathies of unknown origin. Oncol Lett. 2018; 15: 6991–9.
7. Strand DS, Jeffus SK, Sauer BG, Wang AY, Stelow EB, Shami VM. EUS guided 22-gauge fine needle aspiration versus core biopsy needle in the evaluation of solid pancreatic neoplasms. Diagn Cytopathol. 2014; 42: 751–8.
8. Mehmood S, Loya A, Yuduf MA. Clinical utility of endoscopic ultrasound guided fine needle aspiration in the diagnosis of mediastinal and intra-abdominal lymphadenopathy. Acta Cytol. 2013; 57: 436–42.
9. Jhala NC, Jhala D, Eltoum I, et al. Endoscopic ultrasound guided fine needle aspiration biopsy: A powerful tool to obtain samples from small lesions. Cancer. 2004; 102: 239–46.
10. Okasha H, Elkholy S, Sayed M, et al. Ultrasound endoscopic elastography, and the strain ratio in differentiating benign from malignant lymph nodes. Arab J Gastroenterol. 2018; 19: 7–15.
11. Chen VK, Eloubeidi MA. Endoscopic ultrasound-guided fine needle aspiration is superior to lymph node echofeatures: A prospective evaluation of mediastinal and peri-intestinal lymphadenopathy. Am J Gastroenterol. 2004; 99: 628–33.
12. Meda BA, Buss DH, Woodruff RD, et al. Diagnosis and subclassification of primary and recurrent lymphoma. The usefulness and limitations of combined fine-needle aspiration cytomorphology and flow cytometry. Am J Clin Pathol. 2000; 113: 688–99.
13. Young NA, Al-Saleem TI, Ehya H, Smith MR. Utilization of fine needle aspiration cytology and flow cytometry in the diagnosis and subclassification of primary and recurrent lymphoma Cancer. Cancer Cytopathol. 1998; 84: 252–61.
14. Catalano MF, Sivak MJ Jr, Rice T, Gragg LA, Van Dam J. Endoscopic features predictive of lymph node metastasis. Gastrointest Endosc. 1994; 40: 442–6.
15. Savides TJ. Tricks for improving EUS-FNA accuracy and maximizing cellular yield. Gastrointest Endosc. 2009; 69: S130–S133.
16. ASGE standards of practice committee, Early DS, Acosta RD, Chabdrasekhara V, et al. Adverse events associated with EUS and EUS with FNA. Gastroindest Endosc. 2013; 77: 839–43.
17. Chin YK, Iglecias-Garcia J, Iglesia D, et al. Accuracy of endoscopic ultrasound guided tissue acquisition in the evaluation of lymph nodes enlargement in the absence of on-site pathologist. World J Gastroenterol 2017; 23(31): 5755–63.
18. Collins JA, Novak A, Ali SZ, Olson M. Cytotechnologists and on-site evaluation of adequacy. Korean J Pathol. 2013; 47: 405–10.
19. Chand P, Amit S, Gupta R, Agrawal A. Errors, limitations, and pitfalls in the diagnosis of central and peripheral nervous system lesions in intraoperative cytology and frozen sections. J Cytol. 2016; 33(2): 93–7.
20. Nasir H, Haque AUI. Value of touch preparation cytology in intraoperative consultation diagnosis of astrocytomas. International J Pathol. 2003; 1: 8–12.
21. Hamasaki M, Chang KHF, Nabeshima K, Tauchi-Nishi PS. Intraoperative squash and touch preparation cytology of brain lesions stained with H&E and Diff-Quik: A 20-year retrospective analysis and comparative literature review. Acta Cytol. 2018; 62(1): 44–53.
22. Qiao N, Swearingen B, Hedley-Whyte ET, Tritos NA. The utility of intraoperative cytological smear and frozen section in the surgical management of patients with Cushing's Disease due to Pituitary Microadenomas. Endocr Pathol. 2019; 30(3): 180–8.
23. Jindal A, Diwan H, Kaur K, Sinha VD. Intraoperative Squash Smear in Central Nervous System Tumors and its correlation with Histopathology: 1 year study at a tertiary care centre. J Neurosci Rural Pract. 2017; 8(2): 221–4.
24. Khuroo MS, Hamdani SM, Alam SS, Safar BR, Dar NQ, Bhat RA. Accuracy and utility of intyraoperative wquash smear cytology in neurosurgical practice. Int J Med Sci Public Health. 2019; 8(2): 130–5.
25. Lin O, Rudomina D, Feratovic R, Sirintrapun SJ. Rapid on-site evaluation using telecytology: A major cancer center experience. Diagn Cytopathol. 2019 Jan; 47(1): 15–9.

Peritendinitis of the Fourth Dorsal Compartment Due to Anomalous Extensor Indicis Proprius: A Case Report and Review of Anatomical Variations

Dimas Drummond[1], José Luiz Masson de Almeida Prado[2], Henrique Shimidu[3], Márcio Luís Duarte[4,*]

ABSTRACT

Anomalous extensor indicis proprius (EIP) tendons are rare anatomical variations that can cause wrist pain and dysfunction due to tendon compression and inflammation. These variations, though often asymptomatic, are implicated in conditions such as fourth extensor compartment peritendinitis, requiring accurate diagnosis and tailored treatment. We report the case of a 56-year-old man with chronic right wrist pain lasting eight months, primarily aggravated by finger extension. Physical examination revealed a tender nodule on the dorsum of the wrist and pain elicited by the Spinner test, indicating involvement of the fourth dorsal compartment. Magnetic resonance imaging (MRI) showed an anomalous, thickened EIP tendon with peritendinitis. The patient opted for conservative management, including nonsteroidal anti-inflammatory drugs (NSAIDs) and activity modification, which led to complete symptom resolution within two weeks. This case highlights the clinical relevance of EIP tendon anomalies, which can mimic other wrist pathologies. The Spinner test and imaging modalities such as MRI are essential for diagnosis. While conservative treatment is often sufficient, surgical decompression may be necessary in refractory cases. Awareness of these rare anatomical variations is crucial for accurate diagnosis and effective management, ensuring better outcomes for patients with wrist pain.

KEYWORDS

anomalous extensors; wrist pain; extensor indicis proprius

AUTHOR AFFILIATIONS

[1] Universidade de Ribeirão Preto – Campus Guarujá, Guarujá-SP, Brazil
[2] Fleury Medicina e Saúde, São Paulo-SP, Brazil
[3] Hospital Samaritano, São Paulo-SP, Brazil
[4] Universidade de Ribeirão Preto – Campus Guarujá, Guarujá-SP, Brazil. Diagnósticos da América S/A – DASA, São Paulo-SP, Brazil
* Corresponding author: Universidade de Ribeirão Preto (UNAERP) – Campus Guarujá, Av. D. Pedro I, 3.300, Enseada, Guarujá-SP, Brazil; e-mail: marcioluisduarte@gmail.com

Received: 24 December 2024
Accepted: 12 August 2025
Published online: 6 October 2025

Acta Medica (Hradec Králové) 2025; 68(2): 73–75
https://doi.org/10.14712/18059694.2025.23

INTRODUCTION

The extensor indicis (EI) muscle originates from the posterior surface of the ulna and inserts into the index finger (1). Anatomical variations, such as the anomalous extensor indicis proprius (EIP), are rare but can cause hand pain and dysfunction due to compression and inflammation of adjacent tendons, resulting in wrist pain. Although these variants rarely cause symptoms, several published reports have linked them to cases of wrist pain (2).

The evolution of forearm extensor muscles involves three main groups: brachio-antebrachial, antebrachial-manual, and manual. Anatomical variations, such as the *extensor indicis et medii communis* (EIMC) and *extensor digitorum brevis manus* (EDBM), have incidences ranging from 1% to 12%. Although rare, these anomalies can cause dorsum hand pain and are suspected through clinical tests (3).

Here, we report the case of a 56-year-old man with right wrist pain for eight months treated conservatively.

CASE REPORT

A 56-year-old man presented with a history of chronic right wrist pain persisting for eight months. The discomfort was most pronounced during finger extension and had progressively interfered with his daily activities. He described the pain as localized to the dorsum of the wrist, with exacerbation during specific movements.

On physical examination, a palpable and tender nodule was identified on the dorsum of the wrist. The Spinner test, which involves wrist flexion and metacarpophalangeal joint extension of the index finger against resistance, elicited significant pain localized to the fourth dorsal compartment. Besides localized tenderness and pain provoked by the Spinner test, there was no snapping wrist phenomenon, no palpable crepitus, and no clinical evidence of extensor tendon subluxation. Posterior interosseous nerve entrapment was considered; however, the pain was strictly localized to the dorsal wrist, there were no neurological deficits (including preserved finger and thumb extension strength), and imaging demonstrated tenosynovial inflammation at the fourth compartment – findings that favored a tendinous etiology over neuropathic pain. This finding was consistent with tendon pathology. The patient denied any history of prior surgeries, trauma, or systemic illnesses, with no other relevant medical history.

Magnetic resonance imaging (MRI) of the wrist revealed key diagnostic findings, including fluid effusion within the sheath of the common extensor tendons of the fingers. Additionally, the imaging showed a thickened, anomalous extensor indicis proprius (EIP) tendon with intermediate signal intensity and surrounding fluid, indicative of inflammation. Although the MRI confirmed the anomalous tendon within the fourth dorsal compartment, the distal insertions and potential bifurcations were not fully covered in the protocol, preventing a definitive classification according to Komiyama et al. (1). Therefore, it was reported simply as an anomalous EIP associated with peritendinitis. These findings confirmed the diagnosis of peritendinitis of the fourth extensor compartment, attributed to degeneration of the anomalous EIP tendon (Fig. 1).

Given the absence of significant functional impairment or severe symptoms, the patient opted for conservative management over surgical intervention. He was prescribed a regimen of nonsteroidal anti-inflammatory drugs (NSAIDs) and advised on activity modification to alleviate mechanical stress on the affected tendons. Remarkably, his symptoms resolved completely within two weeks, demonstrating a favorable response to conservative treatment.

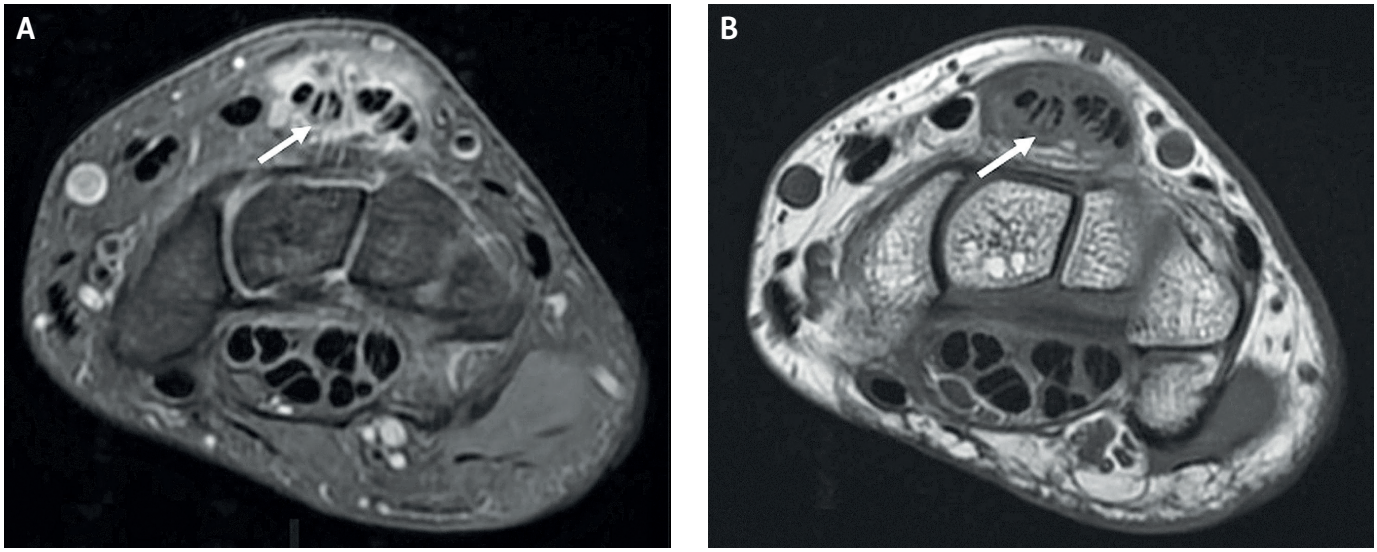

Fig. 1 Right wrist MRI DP FAT SAT sequence (A) and T1 sequence (B) in axial section detecting fluid effusion in the sheath of the common extensor tendons of the fingers, and a thickened anomalous extensor indicis proprius (EIP) tendon with intermediate signal and surrounding fluid effusion, characterizing peritendinitis of the fourth extensor compartment due to a degenerated anomalous EIP tendon (white arrows). The set of findings is compatible with extensor index finger syndrome.

Informed consent for the publication of this case report and accompanying images was obtained from the patient.

DISCUSSION

In 1939, Garcia highlighted the clinical significance of anomalous EIP of the hand (4). EIP syndrome was initially defined by Ritter and Inglis in 1969, who reported two patients with dorsal wrist pain and localized swelling in the fourth compartment. Surgical exploration revealed marked synovitis and a distal muscle belly of the EIP (5).

In Komiyama et al.'s study of 164 hands, 87% of cases showed the EI tendon inserting on the ulnar side of the extensor digitorum (ED) tendon for the index finger, considered the normal type. In 13% of hands, anatomical variations were classified into four types. Type 1 involved tendon bifurcation into two slips. Type 2 showed additional tendons, while Type 3 presented an extra tendon on the ulnar side, inserting into the middle finger. An index extensor muscle with three tendons originating from the muscle was classified as Type 4. In this type, a radial index extensor from the supernumerary tendons was positioned on the radial side of the ED tendon for the index finger and attached to the radial side of the dorsum of this finger (1).

In our case, MRI localized the pathology to an anomalous EIP within the fourth dorsal compartment but did not allow definitive Komiyama subtyping. In the event of failed conservative therapy, the preferred operation would be open decompression with tenosynovectomy. Intraoperative inspection is crucial to identify and, if necessary, address any accessory slip or low-lying tendon/muscle belly (e.g., selective debulking or resection), thereby relieving compartment crowding and reducing the risk of recurrence while preserving index extension.

The EIP muscle presents anatomical variations in 15.6% of cases, as evidenced by Caudwell et al. (6). Ogura et al. suggest that the extensor digitorum brevis manus (EDBM) may be a variant of the EIP, with an incidence of up to 10% (7). Although rare, these anomalies can cause pain on the dorsum of the hand (8).

The Spinner test, developed in 1972, aids in diagnosing EIP syndrome, provoking pain in the fourth dorsal compartment when the wrist is flexed and the index finger extended against resistance. The pain intensifies with simultaneous flexion of the wrist and the metacarpophalangeal joint of the index finger, occurring both with active and passive flexion. EIP syndrome was described by Ritter and Inglis in 1969, characterized by pain and localized swelling on the dorsum of the wrist, with synovitis and tendon changes (9).

Ultrasonography may aid in diagnosis. In the report of Kim 2013, the anomalous extensor muscle was identified showing a typical muscle-like echo texture (10). Diagnosis can be assisted by MRI and should consider anatomical variations, accessory insertions of the EIP tendon, accessory finger muscles, ganglia, and synovitis (11). The Spinner and Olshansky test aids in diagnosing EIP syndrome, which is initially treated conservatively, consisting of rest, splinting, and steroid injection as the initial therapy (12). Surgical decompression of the fourth compartment is an option if conservative treatment fails (13). Although posterior interosseous neuropathy can present with dorsal forearm pain, our patient lacked neurological deficits and had focal fourth-compartment tenosynovitis, making nerve compression unlikely in this context.

CONCLUSION

This case report highlights the importance of recognizing muscle anomalies, such as an anomalous extensor indicis proprius tendon, which can lead to complications such as fourth extensor compartment peritendinitis. Identifying anatomical variations is crucial, as it can directly impact the diagnosis and treatment of painful wrist conditions. Although conservative treatment with nonsteroidal anti-inflammatory drugs was effective in this case, it is essential to consider surgical options in situations where conservative management does not provide relief. Careful clinical evaluation, combined with the use of imaging techniques such as magnetic resonance imaging, can facilitate the differentiation between similar conditions, contributing to a more targeted therapeutic approach. This case reinforces the need for a deeper understanding of wrist muscle anomalies in clinical practice, promoting more accurate diagnosis and appropriate treatments.

REFERENCES

1. Komiyama M, Nwe TM, Toyota N, Shimada Y. Variations of the extensor indicis muscle and tendon. J Hand Surg Br. 1999 Oct; 24(5): 575–8.
2. Baker J, Gonzalez MH. Snapping wrist due to an anomalous extensor indicis proprius: a case report. Hand (NY). 2008 Dec; 3(4): 363–5.
3. Yoshida Y. Anatomical studies on the extensor pollicis et indicis accessorius muscle and the extensor indicis radialis muscle in Japanese. Okajimas Folia Anat Jpn. 1995 Mar; 71(6): 355–63.
4. Garcia AL. Diagnostico erroneo de ganglion carpiano, debido a un musculo supernumerasis. Med Ibera. 1936; 1: 822–4 [Spanish].
5. Ritter MA, Inglis AE. The extensor indicis proprius syndrome. J Bone Joint Surg Am. 1969 Dec; 51(8): 1645–8.
6. Caudwell EW, Anson BJ, Wright RR. The extensor indicis proprius muscle: A study of 263 consecutive specimens. Q Bull Northwest Univ Med Sch. 1943; 17: 267–79.
7. Ogura T, Inoue H, Tanabe G. Anatomic and clinical studies of the extensor digitorum brevis manus. J Hand Surg Am. 1987 Jan; 12(1): 100–7.
8. Reeder CA, Pandeya NK. Extensor indicis proprius syndrome secondary to an anomalous extensor indicis proprius muscle belly. J Am Osteopath Assoc. 1991 Mar; 91(3): 251–3.
9. Li J, Ren ZF. Bilateral extensor medii proprius with split tendon of extensor indicis proprius, a rare anatomical variant. Rom J Morphol Embryol. 2013; 54(3): 639–41.
10. Kim CH. Anomalous extensor indicis proprius muscle. Arch Plast Surg. 2013 Jan; 40(1): 79–81.
11. Patel MR, Moradia VJ, Bassini L, Lei B. Extensor indicis proprius syndrome: a case report. J Hand Surg Am. 1996 Sep; 21(5): 914–5.
12. Yoon C, Hadavi C, Engler A, Erlich M, Mishall P, Pinkas A. Anomalous Extensor Indicis Proprius Muscle Extending Beyond the Extensor Retinaculum: A Case Report. JBJS Case Connect. 2023 Feb 22; 13(1): e22.00681.
13. Tan ST, Smith PJ. Anomalous extensor muscles of the hand: a review. J Hand Surg Am. 1999 May; 24(3): 449–55.